

PRECONDITIONED DISCONTINUOUS GALERKIN METHOD FOR ELLIPTIC INTERFACE PROBLEM ON UNFITTED MESH WITH RECONSTRUCTED DISCONTINUOUS APPROXIMATION

RUO LI, QICHENG LIU, FANYI YANG, AND SHUHAI ZHAO

ABSTRACT. In this paper, we develop an efficient preconditioned unfitted finite element method for the elliptic interface problem, based on the reconstructed discontinuous approximation. The approximation method for interface problems is originally proposed in [Li et al. SIAM J. Sci. Comput. 42(2), 2020], in which an arbitrarily high-order approximation space with one degree of freedom per element is constructed by solving least squares fitting problems. The space can be applied within the cut discontinuous Galerkin framework, where the jump conditions across the interface are weakly enforced by the Nitsche's penalty method. In this work, the local least squares problem is modified by introducing appropriate constraints, which allows us to naturally ensure the stability near the interface by the reconstructed space, and further enables us to establish a norm equivalence between the high-order space and the lowest-order space. This equivalence property motivates us to construct a preconditioner from the piecewise constant space, and this preconditioning method is shown to be optimal in the sense that the upper bound of the condition number to the preconditioned system is independent of the mesh size, the coefficient and the interface location relative to the unfitted mesh. We also present the multigrid algorithms that serve as the inverse of the lowest-order system matrix. Numerical experiments in both two and three dimensions confirm the optimal convergence rates under error measurements and illustrate the efficiency and the robustness of the preconditioning method.

keywords: elliptic interface problem; unfitted mesh; cut finite element method; reconstructed discontinuous approximation; multigrid preconditioning;

1. INTRODUCTION

The interface problems serve as fundamental models for a wide range of physical phenomena involving multiple materials or media. The governing equations are usually coupled via jump conditions imposed across the interface. As a prototypical example, the elliptic interface problem arises in numerous scientific and engineering applications, including material sciences, porous media flow and the multiphase flow [15, 33, 11]. Consequently, the development of numerical methods for elliptic interface problems has attracted considerable research attention in recent years.

Finite element methods (FEM) are widely used for solving elliptic interface problems, which can be roughly classified into body-fitted methods and body-unfitted methods. In body-fitted methods, the interfaces are required to align with grid lines, and thus the generation of body-fitted meshes for complex geometries and interfaces is very challenging and time-consuming. We refer to [15, 6] for some implementations of body-fitted approaches. In contrast, the body-unfitted methods have become popular in recent years, as the mesh generation is completely decoupled from the geometry description of the interface, which provides great flexibility in handling the complex geometries. Li proposed the immersed finite element method (IFEM) for the elliptic interface problem in [41], which now represent a canonical class of unfitted methods. The main idea of this method is to handle the discontinuity of the solution by locally modifying the basis functions or adding some partial penalty terms on cut elements; we refer to [3, 42, 50, 13, 20] for more details. Another typical unfitted method is the cut finite element method (CutFEM), also known as the Nitsche-type extended finite element method (Nitsche-XFEM), proposed by Hansbo and Hansbo in [24]. This method solves the interface

problem with two separate finite element spaces defined on each subdomain, where the jump conditions are weakly enforced by the Nitsche penalty technique. This idea has been applied in many interface problems; see [25, 23, 9, 10, 43, 34, 52] for some applications. For penalty methods, the small cuts near the interface must be treated carefully. Otherwise, the condition number of the resulting linear system cannot be uniformly bounded and the convergence may even deteriorate. Generally, certain stabilization strategies are required, such as the ghost penalty method, the agglomeration of elements and local extension techniques; we refer to [7, 21, 29, 5, 45, 27, 8] for some works. As standard FEM, the discretization usually yields a linear system with the condition number of $O(h^{-2})$ after stabilization. Although the condition number is uniformly bounded, the linear system is still ill-conditioned when the mesh size tends to zero. To the best of our knowledge, there are few works on the (multigrid type) preconditioning method for unfitted methods, especially for high-order schemes. In [32], a preconditioner for the original Nitsche-type finite element method [24] in two dimensions is proposed, which relies on a stable subspace splitting of the linear spaces. In [44], a multigrid preconditioner is proposed for the stabilized Nitsche-type finite element method, where the prolongation operator is specially designed for the nonnested hierarchy of unfitted finite element spaces. This method is also established on linear spaces and the rigorous analysis of the spectral quality of the preconditioner is missing [19]. The multigrid methods for IFEM can be found in [16, 1]. We also refer to [19, 4] for some studies on domain decomposition methods.

In this paper, we propose a preconditioned discontinuous Galerkin (DG) method on unfitted meshes for the elliptic interface problem, based on the reconstructed discontinuous approximation. In this method, a high-order approximation space is reconstructed by solving local least squares fitting problem on every element patch, with only one degree of freedom per element [36, 38, 35]. This space is a subspace of the standard DG space and can inherit the DG schemes and their flexibility while significantly reducing the number of degrees of freedom. This approximation method was applied to the elliptic interface problem in [39]. In this paper, the local least squares fitting problem is modified by adding appropriate constraints, and it is noted these constraints are essential in our scheme. The modification first enables us to establish the norm equivalence property from the physical domain to the active mesh for the reconstructed space without additional stabilization mechanisms. We thus prove that the numerical solution achieves optimal convergence rates under error measurements and the resulting discrete linear system has a condition number of $O(h^{-2})$. Second, the reconstructed space maintains the same dimension regardless of the polynomial degree, which motivates us to construct a preconditioner from the lowest-order space, i.e., the piecewise constant space. By the local constraints, we prove a spectral equivalence between the lowest-order space and any high-order space, and we further show that the preconditioning method is optimal in the sense that the condition number of the preconditioned linear system is independent of the mesh size, the coefficient in the problem and how the interface cuts the unfitted mesh. The low-order preconditioning techniques in standard finite element methods to precondition the high-order matrix can be found in [14, 47, 46]. Typically, the low-order matrix is constructed on a much finer mesh to match the dimension of the high-order matrix. In our method, both high-order and lowest-order matrices are assembled on the same mesh, avoiding the need for any mesh refinement operator. Consequently, the inverse of the matrix arising from the lowest-order system can serve as an optimal preconditioner for the high-order scheme. For the lowest-order scheme, we follow the idea of the smoothed aggregation method [48] to develop the multigrid algorithm, based on a series of successively refined unfitted meshes. The convergence of the multigrid algorithm is also established for the piecewise constant space. Numerical tests in two and three dimensions confirm the accuracy of the proposed scheme and the efficiency of the preconditioning method. As a numerical observation, our method achieves comparable numerical error with fewer degrees of freedom compared to the cut discontinuous Galerkin method. Furthermore, the numerical results demonstrate the robustness of both the scheme and the preconditioning method in the case of coefficients involving large jumps.

The rest of this paper is organized as follows. In Section 2, the notation related to the mesh and the interface is given. In Section 3, we introduce the reconstructed approximation space and present the basic properties of the space. In Section 4, we present the penalty schemes for the elliptic interface problem, along with the corresponding error estimation under the energy norm and the L^2 norm. The stability near the interface is also verified in this section. Section 5 is devoted to the preconditioning method. We prove a norm equivalence between the high-order space and the lowest-order space on the same mesh. For the lowest-order linear system, we present two multigrid algorithms, which can serve as the preconditioner for the high-order linear system. Finally, in Section 6 we conduct a series of numerical experiments in two and three dimensions to validate the accuracy of the proposed scheme and the efficiency of the preconditioning method.

2. PROBLEM SETTING AND PRELIMINARIES

Let $\Omega \subset \mathbb{R}^d (d = 2, 3)$ be a convex polygonal (polyhedral) domain with the boundary $\partial\Omega$. Let $\Omega_0 \Subset \Omega$ be an open subdomain with C^2 -smooth boundary $\partial\Omega_0$. We define $\Gamma := \partial\Omega_0$ as its topological boundary, which can be regarded as a smooth interface dividing Ω into two disjoint subdomains. Let $\Omega_1 := \Omega \setminus \overline{\Omega_0}$, and we have that $\Omega_0 \cap \Omega_1 = \emptyset$ and $\overline{\Omega_0} \cup \overline{\Omega_1} = \overline{\Omega}$. The problem concerned in this paper is the elliptic interface problem, which seeks the solution u such that

$$(1) \quad \begin{aligned} -\nabla \cdot (\alpha \nabla u) &= f, & \text{in } \Omega_0 \cup \Omega_1, \\ u &= g, & \text{on } \partial\Omega, \\ [u] &= a \mathbf{n}_\Gamma, \quad [\alpha \nabla u] = b, & \text{on } \Gamma, \end{aligned}$$

where α is a piecewise positive constant function in $\Omega_0 \cup \Omega_1$ that may be discontinuous across the interface, i.e., $\alpha_i := \alpha|_{\Omega_i} > 0$. The jump operators are defined as (3). For the data functions $f \in L^2(\Omega)$, $g \in H^{3/2}(\partial\Omega)$ and the jump conditions $a \in H^{3/2}(\Gamma)$ and $b \in H^{1/2}(\Gamma)$, the elliptic interface problem admits a unique solution $u \in H^2(\Omega_0 \cup \Omega_1)$. We refer to [31, 26] for more details about the regularity results.

Let \mathcal{T}_h be a quasi-uniform partition of Ω into a series of simplexes (triangles, tetrahedrons). For any $K \in \mathcal{T}_h$, we denote by h_K the diameter of K and by ρ_K the radius of the largest ball inscribed in K . Let $h := \max_{K \in \mathcal{T}_h} h_K$ be the mesh size and set $\rho := \min_{K \in \mathcal{T}_h} \rho_K$. The quasi-uniformity of \mathcal{T}_h reads: there exists a constant C_ν independent of h such that $h \leq C_\nu \rho$. For any $K \in \mathcal{T}_h$, we define $\Delta_K := \{K' \in \mathcal{T}_h : \overline{K'} \cap \overline{K} \neq \emptyset\}$ as the collection of the elements sharing a common vertex with K , and we define Δ_K^s as the set formed by neighbouring elements of layer s in a recursive manner. We initialize $\Delta_K^1 := \Delta_K$ and define $\Delta_K^s := \bigcup_{K' \in \Delta_K^{s-1}} \Delta_{K'}$ for $s \geq 2$. Since \mathcal{T}_h is quasi-uniform, there exists a constant C_Δ depending on C_ν such that $K' \subset B(\mathbf{x}_K, sC_\Delta h_K) (\forall K' \in \Delta_K^s)$, where $B(\mathbf{z}, r)$ denotes the disk (ball) centered at \mathbf{z} with the radius r , and \mathbf{x}_K is the barycenter of K . Let \mathcal{E}_h be the set of all $d-1$ dimensional faces of \mathcal{T}_h , and we decompose \mathcal{E}_h into $\mathcal{E}_h = \mathcal{E}_h^I \cup \mathcal{E}_h^B$, where \mathcal{E}_h^I and \mathcal{E}_h^B are collections of all interior faces and faces lying on the boundary $\partial\Omega$, respectively. The faces in \mathcal{E}_h are not required to be aligned with Γ . For any $e \in \mathcal{E}_h$, we denote by h_e the diameter of the face e .

We further give the notation related to the subdomains $\Omega_i (i = 0, 1)$. Let

$$\mathcal{T}_{h,i} := \{K \in \mathcal{T}_h \mid K \cap \Omega_i \neq \emptyset\}, \quad \mathcal{T}_{h,i}^\circ := \{K \in \mathcal{T}_{h,i} \mid K \subset \Omega_i\}, \quad \mathcal{T}_h^\Gamma := \{K \in \mathcal{T}_h \mid K \cap \Gamma \neq \emptyset\},$$

where $\mathcal{T}_{h,i}$ is the minimal set of elements completely covering the whole domain Ω_i , and $\mathcal{T}_{h,i}^\circ$ is the set of all interior elements inside Ω_i , and \mathcal{T}_h^Γ is the set of all cut elements. We define $\Omega_{h,i} := \text{Int}(\bigcup_{K \in \mathcal{T}_{h,i}} \overline{K})$, $\Omega_{h,i}^\circ := \text{Int}(\bigcup_{K \in \mathcal{T}_{h,i}^\circ} \overline{K})$, $\Omega_h^\Gamma := \text{Int}(\bigcup_{K \in \mathcal{T}_h^\Gamma} \overline{K})$ as their corresponding domains. For the partition $\mathcal{T}_{h,i}$, we let $\mathcal{E}_{h,i}$ be the set of all $d-1$ dimensional faces in $\mathcal{T}_{h,i}$, and we let $\mathcal{E}_{h,i}^I \subset \mathcal{E}_{h,i}$ be the set of all interior faces inside $\Omega_{h,i}$. For any $K \in \mathcal{T}_h$ and any $e \in \mathcal{E}_h$, we define $K^i := K \cap \Omega_i$ and $e^i := e \cap \Omega_i$. For any cut element $K \in \mathcal{T}_h^\Gamma$, we define $\Gamma_K := K \cap \Gamma$.

We make the following geometrical assumption about the mesh.

Assumption 1. *There exists a constant s_0 such that there exist two injective relation mappings $(\cdot)^{\sigma_i} (i = 0, 1) : \mathcal{T}_h^\Gamma \rightarrow \mathcal{T}_{h,i}^\circ$ satisfying $K^{\sigma_i} \in \Delta_K^s \cap \mathcal{T}_{h,i}^\circ$ with an index $s \leq s_0$ for $\forall K \in \mathcal{T}_h^\Gamma$.*

For $i = 0, 1$, since $(\cdot)^{\sigma_i}$ is required to be injective, $K_-^{\sigma_i} \neq K_+^{\sigma_i}$ for different $K_-, K_+ \in \mathcal{T}_h^\Gamma$. Let $\mathcal{T}_{h,i}^{\Gamma,1} := \bigcup_{K \in \mathcal{T}_h^\Gamma} (\Delta_K^1 \cap \mathcal{T}_{h,i}^\circ)$ and $\mathcal{T}_{h,i}^{\Gamma,2} := \bigcup_{K \in \mathcal{T}_h^\Gamma} (\Delta_K^2 \cap \mathcal{T}_{h,i}^\circ)$. Because Γ is of C^2 , roughly speaking, there will be $2\#\mathcal{T}_h^\Gamma \approx 2\#\mathcal{T}_{h,i}^{\Gamma,1} \approx \#\mathcal{T}_{h,i}^{\Gamma,2}$ for a sufficiently fine mesh. Hence, the set $\mathcal{T}_{h,i}^{\Gamma,2}$ contains many more elements than \mathcal{T}_h^Γ . This fact allows us to seek the unique K^{σ_i} in $\Delta_K^2 \cap \mathcal{T}_{h,i}^\circ$ for $\forall K \in \mathcal{T}_h^\Gamma$, and generally there holds $s_0 = 2$ in Assumption 1. In the computer implementation, for every $K \in \mathcal{T}_h^\Gamma$, if there exists an element $K' \in \Delta_K^1 \cap \mathcal{T}_{h,i}^\circ$ that has not been marked, then we let $K^{\sigma_i} = K'$ and mark K' ; otherwise, we choose any element $K' \in \Delta_K^2 \cap \mathcal{T}_{h,i}^\circ$ that has not been marked as K^{σ_i} . We further define the set $\mathcal{T}_{h,i}^{\Gamma,\circ}$ as $\mathcal{T}_{h,i}^{\Gamma,\circ} := \{K' \in \mathcal{T}_{h,i}^\circ : \exists K \in \mathcal{T}_h^\Gamma \text{ such that } K^{\sigma_i} = K'\}$. For any $K' \in \mathcal{T}_{h,i}^{\Gamma,\circ}$, we formally define an inverse mapping $(\cdot)^{\varsigma_i}$ by letting $(K')^{\varsigma_i} := K \in \mathcal{T}_h^\Gamma$ such that $K^{\sigma_i} = K'$.

Let us introduce the jump and average operators adopted in the numerical scheme. Let v and \mathbf{q} be the piecewise smooth scalar- and vector-valued function on $\mathcal{T}_{h,i} (i = 0, 1)$. For any interior face $e \in \mathcal{E}_{h,i}^I$, we let $e = \partial K^+ \cap \partial K^-$ be shared by two neighbouring elements $K^+, K^- \in \mathcal{T}_{h,i}$, and we let $\mathbf{n}^+, \mathbf{n}^-$ be the unit outward normal vector on The jump operators $[\cdot]$ and the average operators $\{\cdot\}$ on e are defined as

$$\begin{aligned} [v]|_e &:= v^+|_e \mathbf{n}^+ + v^-|_e \mathbf{n}^-, & [\mathbf{q}]|_e &:= \mathbf{q}^+|_e \cdot \mathbf{n}^+ + \mathbf{q}^-|_e \cdot \mathbf{n}^-, \\ \{v\}|_e &:= \frac{1}{2}(v^+|_e + v^-|_e), & \{\mathbf{q}\}|_e &:= \frac{1}{2}(\mathbf{q}^+|_e + \mathbf{q}^-|_e), \end{aligned} \quad \forall e \in \mathcal{E}_{h,i}^I,$$

where $v^\pm := v|_{K^\pm}$, $\mathbf{q}^\pm := \mathbf{q}|_{K^\pm}$. For the face $e \in \mathcal{E}_h^B$, we let \mathbf{n} be the unit outward normal vector on e , and the trace operators are given as

$$[v]|_e := v|_e \mathbf{n}, \quad [\mathbf{q}]|_e := \mathbf{q}|_e \cdot \mathbf{n}, \quad \{v\}|_e := v|_e, \quad \{\mathbf{q}\}|_e := \mathbf{q}|_e, \quad \forall e \in \mathcal{E}_h^B.$$

For any cut element $K \in \mathcal{T}_h^\Gamma$, we let v and \mathbf{q} be the scalar- and vector-valued function that may be discontinuous across Γ_K . In this paper, we use the following harmonic weights as adopted in DG methods [12, 27, 18] to obtain the robustness for coefficients with large jumps:

$$(2) \quad w^0 := \frac{\alpha_1}{\alpha_0 + \alpha_1}, \quad w^1 := \frac{\alpha_0}{\alpha_0 + \alpha_1}, \quad \{\alpha\}_w = \frac{2\alpha_0\alpha_1}{\alpha_0 + \alpha_1},$$

where $\alpha_{\min} \leq \{\alpha\}_w \leq \alpha_{\max}$, $\{\alpha\}_w \leq 2\alpha_{\min}$ with $\alpha_{\min(\max)} := \min(\max)(\alpha_0, \alpha_1)$. The jump and the average operators on the interface are defined as

$$(3) \quad \begin{aligned} [v]|_{\Gamma_K} &:= (v^0|_{\Gamma_K} - v^1|_{\Gamma_K}) \mathbf{n}_\Gamma, & [\mathbf{q}]|_{\Gamma_K} &:= (\mathbf{q}^0|_{\Gamma_K} - \mathbf{q}^1|_{\Gamma_K}) \cdot \mathbf{n}_\Gamma, \\ \{v\}_w|_{\Gamma_K} &:= w^0 v^0|_{\Gamma_K} + w^1 v^1|_{\Gamma_K}, & \{\mathbf{q}\}_w|_{\Gamma_K} &:= w^0 \mathbf{q}^0|_{\Gamma_K} + w^1 \mathbf{q}^1|_{\Gamma_K}, \quad \forall K \in \mathcal{T}_h^\Gamma, \\ \{v\}^w|_{\Gamma_K} &:= w^1 v^0|_{\Gamma_K} + w^0 v^1|_{\Gamma_K}, & \{\mathbf{q}\}^w|_{\Gamma_K} &:= w^1 \mathbf{q}^0|_{\Gamma_K} + w^0 \mathbf{q}^1|_{\Gamma_K}, \end{aligned}$$

where $v^i := v|_{K^i}$, $\mathbf{q}^i := \mathbf{q}|_{K^i}$, and \mathbf{n}_Γ denotes the unit normal vector on Γ pointing from Ω_0 to Ω_1 .

For a bounded domain D , $H^r(D)$ denotes the usual Sobolev spaces with the regular exponent $r \geq 0$, and the standard definitions to the inner products, seminorms and norms of $H^r(D)$ are also followed. For $r = 0$, the space $H^0(D)$ coincides with the space $L^2(D)$. Throughout this paper, C and $C_i (i = 0, 1, \dots)$ are denoted as generic constants that may vary in different occurrences but are always independent of h , the coefficient α and how the interface Γ intersects the mesh \mathcal{T}_h . In the error estimation, we need the Sobolev extension theory and the H^1 trace estimate on the interface. For $i = 0, 1$, there exists an extension operator $E^i : H^t(\Omega_i)^d \rightarrow H^t(\Omega)^d (t \geq 2)$ such that [2, Chapter 5]

$$(4) \quad (E^i v)|_{\Omega_i} = v, \quad \|E^i v\|_{H^s(\Omega)} \leq C \|v\|_{H^s(\Omega_i)}, \quad 0 \leq s \leq t, \quad \forall v \in H^t(\Omega_i).$$

The local H^1 trace estimate on the interface reads: there exists a constant C such that [24, 51]

$$(5) \quad \|v\|_{L^2(\Gamma_K)}^2 \leq C (h_K^{-1} \|v\|_{L^2(K)}^2 + h_K \|\nabla v\|_{L^2(K)}^2), \quad \forall v \in H^1(K), \quad \forall K \in \mathcal{T}_h^\Gamma.$$

3. DISCONTINUOUS RECONSTRUCTED APPROXIMATION

In this section, we introduce the approximation space by defining two linear reconstruction operators $\mathcal{R}^{m,i}$ ($i = 0, 1$) in the domain $\Omega_{h,i}$. Let $V_{h,i} := \{v_h \in L^2(\Omega_{h,i}) : v_h|_K \in \mathcal{P}_0(K), \forall K \in \mathcal{T}_{h,i}\}$ be the piecewise constant space over $\mathcal{T}_{h,i}$. The linear operator $\mathcal{R}^{m,i}$ will reconstruct the lowest-order space $V_{h,i}$ into a piecewise high-order polynomial space over $\mathcal{T}_{h,i}$. Following the idea in [39, 40], the construction of $\mathcal{R}^{m,i}$ ($i = 0, 1$) includes two steps.

Step I. We construct a wide element patch \mathcal{S}_K^i for each element in $\mathcal{T}_{h,i}$. The patch consists of some neighbouring elements around K . We prescribe a threshold \mathcal{N}_m to control the size of the patch, and its value will be specified later. Let $\mathcal{S}_{K,s}^i := \Delta_K^s \cap \mathcal{T}_{h,i}$, and we first seek a depth t such that $\#\mathcal{S}_{K,t}^i < \mathcal{N}_m \leq \#\mathcal{S}_{K,t+1}^i$. It is noted that Δ_K^s is defined in a recursive manner, and such t can be readily computed by a recursive algorithm based on the definition of $\mathcal{S}_{K,s}^i$; we denote by $t_{K,m}^i := t$ the recursive depth for K . Then, we sort the elements in $\mathcal{S}_{K,t+1}^i \setminus \mathcal{S}_{K,t}^i$ by their distances to K , where the distance between two elements is measured by the distance between their barycenters. We let $\mathcal{S}_K^i = \mathcal{S}_{K,t}^i$ and add the first $\mathcal{N}_m - \#\mathcal{S}_{K,t}^i$ elements in $\mathcal{S}_{K,t+1}^i \setminus \mathcal{S}_{K,t}^i$ to \mathcal{S}_K^i . As a result, we have collected exactly \mathcal{N}_m elements in \mathcal{S}_K^i , and there holds $\mathcal{S}_K^i \subset \mathcal{T}_{h,i}$. We define $\mathcal{D}_K^i := \text{Int}(\bigcup_{K' \in \mathcal{S}_K^i} \overline{K'})$ as the corresponding domain to the patch. Because $\mathcal{T}_h^\Gamma = \mathcal{T}_{h,0} \cap \mathcal{T}_{h,1}$, each cut element K has two patches \mathcal{S}_K^0 and \mathcal{S}_K^1 , while all interior elements only have one patch.

We make the following assumption on patches, which can be easily fulfilled by selecting a bit large \mathcal{N}_m .

Assumption 2. For any interior element $K \in \mathcal{T}_{h,i}^{\Gamma,\circ}$ ($i = 0, 1$), there holds $K^{\text{si}} \in \mathcal{S}_K^i$.

Step II. Next, we solve a least squares fitting problem per element patch in $\mathcal{T}_{h,i}$. For any $K \in \mathcal{T}_{h,i}$, we define the set

$$\mathcal{C}_K^i := \begin{cases} \{\mathbf{x}_K, \mathbf{x}_{K^{\text{si}}}\}, & \text{for interior } K \in \mathcal{T}_{h,i}^{\Gamma,\circ}, \\ \{\mathbf{x}_K\}, & \text{for cut } K \in \mathcal{T}_{h,i} \setminus \mathcal{T}_{h,i}^{\Gamma,\circ}. \end{cases}$$

Let $v_{h,i} \in V_{h,i}$ be any piecewise constant function on $\mathcal{T}_{h,i}$, and for any $K \in \mathcal{T}_{h,i}$, we solve a constrained least squares problem on each patch \mathcal{S}_K^i , which depends on barycenters of all elements in \mathcal{S}_K^i and the set \mathcal{C}_K^i :

$$(6) \quad \arg \min_{p \in \mathcal{P}_m(\mathcal{D}_K^i)} \sum_{K' \in \mathcal{S}_K^i} (p(\mathbf{x}_{K'}) - v_{h,i}(\mathbf{x}_{K'}))^2, \quad \text{s.t. } p(\mathbf{y}) = v_{h,i}(\mathbf{y}), \quad \forall \mathbf{y} \in \mathcal{C}_K^i.$$

We make the following geometrical assumption to ensure the existence and the uniqueness of the solution to (6).

Assumption 3. For every patch \mathcal{S}_K^i ($\forall K \in \mathcal{T}_{h,i}, i = 0, 1$), any polynomial $p \in \mathcal{P}_m(\mathcal{D}_K^i)$ satisfying $p(\mathbf{x}_K) = 0$ ($\forall K \in \mathcal{S}_K^i$) implies $p \equiv 0$.

By Assumption 3, the prescribed threshold \mathcal{N}_m is required to be greater than $\dim(\mathcal{P}_m)$, and this condition can be readily satisfied by selecting a bit large \mathcal{N}_m in practice. Moreover, the barycenters of elements in \mathcal{S}_K^i are required not to lie on an algebraic curve (surface) of degree m .

Let us show that the solution to the problem (6) is unique.

Lemma 1. For each $K \in \mathcal{T}_{h,i}$ ($i = 0, 1$), the problem (6) admits a unique solution.

Proof. Let p_1 and p_2 be two solutions to (6). Let $q \in \mathcal{P}_m(\mathcal{D}_K^i)$ be any polynomial with $q|_{\mathcal{C}_K^i} = 0$, and thus $p_i + tq$ meets the constraint of (6). We have that

$$\sum_{K' \in \mathcal{S}_K^i} (p_i(\mathbf{x}_{K'}) + tq(\mathbf{x}_{K'}) - v_{h,i}(\mathbf{x}_{K'}))^2 \geq \sum_{K' \in \mathcal{S}_K^i} (p_i(\mathbf{x}_{K'}) - v_{h,i}(\mathbf{x}_{K'}))^2.$$

Since t is arbitrary, the above inequality is equivalent to

$$(7) \quad \sum_{K' \in \mathcal{S}_K^i} q(\mathbf{x}_{K'}) (p_i(\mathbf{x}_{K'}) - v_{h,i}(\mathbf{x}_{K'})) = \sum_{K' \in \mathcal{S}_K^i} q(\mathbf{x}_{K'}) (p_1(\mathbf{x}_{K'}) - p_2(\mathbf{x}_{K'})) = 0.$$

It is noted that $(p_1 - p_2)|_{\mathcal{C}_K^i} = 0$. In (7), taking $q = p_1 - p_2$ immediately yields that $p_1 - p_2$ vanishes at all barycenters of elements in \mathcal{S}_K^i . Then, $p_1 = p_2$ is concluded by Assumption 3, which completes the proof. \square

Let $v_{h,\mathcal{S}_K^i} \in \mathcal{P}_m(\mathcal{D}_K^i)$ be the solution of (6), and it has a linear dependence on the given function $v_{h,i}$. From this fact, we introduce a linear operator $\mathcal{R}_K^{m,i} : V_{h,i} \rightarrow \mathcal{P}_m(\mathcal{D}_K^i)$ by letting $\mathcal{R}_K^{m,i} v_{h,i} := v_{h,\mathcal{S}_K^i}$ for any $v_{h,i} \in V_{h,i}$. Further, it is natural to define a global linear operator $\mathcal{R}^{m,i}$ in a piecewise manner on $\mathcal{T}_{h,i}$,

$$(8) \quad \begin{aligned} \mathcal{R}^{m,i} : V_{h,i} &\rightarrow U_{h,i}^m, \\ v_{h,i} &\rightarrow \mathcal{R}^{m,i} v_{h,i}, \end{aligned} \quad (\mathcal{R}^{m,i} v_{h,i})|_K := (\mathcal{R}_K^{m,i} v_{h,i})|_K, \quad \forall K \in \mathcal{T}_{h,i}.$$

It can be observed that $\mathcal{R}^{m,i} v_{h,i}$ is a piecewise polynomial function of degree m . Let $U_{h,i}^m := \mathcal{R}^{m,i} V_{h,i}$ be the image space, which is a piecewise polynomial space over $\mathcal{T}_{h,i}$. Indeed, the reconstructed space $U_{h,i}^m$ will be used as the approximation space in the scheme to approximate the solution defined in Ω_i .

We will show that the high-order space $U_{h,i}^m$ and the piecewise constant space $V_{h,i}$ have the same dimension.

Lemma 2. *The operator $\mathcal{R}^{m,i}$ ($i = 0, 1$) is full-rank, and $\dim(U_{h,i}^m) = \dim(V_{h,i})$.*

Proof. By the constraint in (6), it follows that $(\mathcal{R}^{m,i} v_{h,i})(\mathbf{x}_K) = v_{h,i}(\mathbf{x}_K)$ for any $v_{h,i} \in V_{h,i}$, which directly implies that $\mathcal{R}^{m,i} v_{h,i} = 0$ for $v_{h,i} \in V_{h,i}$ only if $v_{h,i} = 0$. From the linearity of $\mathcal{R}^{m,i}$, we know that $\mathcal{R}^{m,i}$ is non-degenerate, and thus the dimensions of $V_{h,i}$ and $U_{h,i}^m$ are the same. This completes the proof. \square

We note that the constraints in the problem (6) are essential in our method, which allow us to verify the non-degenerate property of the reconstruction operator, to ensure the stability near the interface and to develop the preconditioning method based on the lowest-order space for our numerical scheme. From Lemma 2, it is straightforward to outline a group of basis functions to the reconstructed space $U_{h,i}^m$. Let $\{e_{K,i}\}_{K \in \mathcal{T}_{h,i}}$ be basis functions of $V_{h,i}$ such that $e_{K,i}(\mathbf{x}_{K'}) = \delta_{K,K'}$ for any $K' \in \mathcal{T}_{h,i}$, and we let $\lambda_{K,i} := \mathcal{R}^{m,i} e_{K,i}$. Since $\mathcal{R}^{m,i}$ is full-rank, there holds $U_{h,i}^m = \text{span}(\{\lambda_{K,i}\}_{K \in \mathcal{T}_{h,i}})$. For $e_{K,i}$, we have that $e_{K,i}|_{\mathcal{D}_{K'}^i} = 0$ for any K' with $K \notin \mathcal{S}_{K'}^i$, which brings $\mathcal{R}_K^{m,i} e_{K,i} = 0$. This fact gives that $\lambda_{K,i}$ is compactly supported by $\text{supp}(\lambda_{K,i}) = \bigcup_{K'|K \in \mathcal{S}_{K'}^i} \overline{K'}$. By $\{e_{K,i}\}_{K \in \mathcal{T}_{h,i}}$, any $v_{h,i} \in V_{h,i}$ has the expansion $v_{h,i} = \sum_{K \in \mathcal{T}_{h,i}} v_{h,i}(\mathbf{x}_K) e_{K,i}$. Hence, $\mathcal{R}^{m,i} v_{h,i}$ admits the following expansion

$$(9) \quad \mathcal{R}^{m,i} v_{h,i} = \sum_{K \in \mathcal{T}_{h,i}} v_{h,i}(\mathbf{x}_K) \lambda_{K,i}, \quad \forall v_{h,i} \in V_{h,i}.$$

From this expansion, the operator $\mathcal{R}^{m,i}$ can be directly extended to the continuous space $C^0(\Omega_{h,i})$. For any $v_{h,i} \in C^0(\Omega_{h,i})$, we define $\mathcal{R}^{m,i} v_{h,i}$ as (9), or equivalently, $\mathcal{R}^{m,i} v_{h,i} = \mathcal{R}^{m,i} \tilde{v}_{h,i}$, where $\tilde{v}_{h,i} \in V_{h,i}$ is determined by $\tilde{v}_{h,i}(\mathbf{x}_K) = v_{h,i}(\mathbf{x}_K)$ for $\forall K \in \mathcal{T}_{h,i}$.

We next focus on the approximation property of the reconstruction operator, which plays an important role in the error estimation. The following constants are defined to measure the stability of

$\mathcal{R}^{m,i}$,

$$(10) \quad \Lambda_m := \max_{i=0,1} \max_{K \in \mathcal{T}_{h,i}} (1 + t_m \Lambda_{m,K,i} \sqrt{\#\mathcal{S}_K^i}), \quad t_m = \max_{i=0,1} \max_{K \in \mathcal{T}_{h,i}} t_{K,m}^i,$$

$$\Lambda_{m,K,i}^2 := \max_{p \in \mathcal{P}_m(\mathcal{D}_K^i)} \frac{\|p\|_{L^2(K)}^2}{h_K^d \sum_{K' \in \mathcal{S}_K^i} (p(\mathbf{x}_{K'}))^2}, \quad \forall K \in \mathcal{T}_{h,i}.$$

We state the following stability result.

Lemma 3. *For $i = 0, 1$, there holds*

$$(11) \quad \|\mathcal{R}_K^{m,i} v_{h,i}\|_{L^2(K)} \leq C \Lambda_m h_K^{d/2} \max_{K' \in \mathcal{S}_K^i} |v_{h,i}(\mathbf{x}_{K'})|, \quad \forall K \in \mathcal{T}_{h,i}, \quad \forall v_{h,i} \in C^0(\Omega_{h,i}) \cup V_{h,i}.$$

Proof. Let $p = \mathcal{R}_K^{m,i} v_{h,i}$, and the constraint of (6) indicates that $p(\mathbf{x}_K) = v_{h,i}(\mathbf{x}_K)$ for $K \in \mathcal{T}_{h,i} \setminus \mathcal{T}_{h,i}^{\Gamma,\circ}$. We define $l(\mathbf{x}) := v_{h,i}(\mathbf{x}_K)$ as the constant function. For $K \in \mathcal{T}_{h,i}^{\Gamma,\circ}$, there holds $p(\mathbf{x}_K) = v_{h,i}(\mathbf{x}_K)$ and $p(\mathbf{x}_{K^s_i}) = v_{h,i}(\mathbf{x}_{K^s_i})$. Note that $|\mathbf{x}_K - \mathbf{x}_{K^e_i}| \geq Ch_K$, we define a linear function $l(\mathbf{x})$ passing through $(\mathbf{x}_K, v_{h,i}(\mathbf{x}_K))$ and $(\mathbf{x}_{K^e_i}, v_{h,i}(\mathbf{x}_{K^e_i}))$ such that $|\nabla l| \leq \frac{|v_{h,i}(\mathbf{x}_K) - v_{h,i}(\mathbf{x}_{K^e_i})|}{|\mathbf{x}_K - \mathbf{x}_{K^e_i}|} \leq Ch_K^{-1} \max_{K' \in \mathcal{S}_K^i} |v_{h,i}(\mathbf{x}_{K'})|$. Let $q := p - l$, which satisfies the constraint in (6) for both cases, and there holds

$$(12) \quad \|l\|_{L^\infty(\mathcal{D}_K^i)} \leq Ct_{K,m}^i h_K |\nabla l| + l(\mathbf{x}_K) \leq Ct_{K,m}^i \max_{K' \in \mathcal{S}_K^i} |v_{h,i}(\mathbf{x}_{K'})|.$$

We bring such q into (7), which immediately yields that $\sum_{K' \in \mathcal{S}_K^i} (p(\mathbf{x}_{K'}) - l(\mathbf{x}_{K'}))(p(\mathbf{x}_{K'}) - v_{h,i}(\mathbf{x}_{K'})) = 0$. This orthogonality property further leads to

$$\sum_{K' \in \mathcal{S}_K^i} (p(\mathbf{x}_{K'}) - l(\mathbf{x}_{K'}))^2 \leq \sum_{K' \in \mathcal{S}_K^i} (l(\mathbf{x}_{K'}) - v_{h,i}(\mathbf{x}_{K'}))^2 \leq C(t_{K,m}^i)^2 \#\mathcal{S}_K^i \max_{K' \in \mathcal{S}_K^i} |v_{h,i}(\mathbf{x}_{K'})|^2,$$

and

$$\begin{aligned} \|p\|_{L^2(K)}^2 &\leq C(\|p - l\|_{L^2(K)}^2 + \|l\|_{L^2(K)}^2) \leq C(\Lambda_{m,K,i}^2 h_K^d \sum_{K' \in \mathcal{S}_K^i} (l(\mathbf{x}_{K'}) - v_{h,i}(\mathbf{x}_{K'}))^2 + h_K^d \|l\|_{L^\infty(K)}^2) \\ &\leq Ch_K^d (\Lambda_{m,K,i}^2 (t_{K,m}^i)^2 \#\mathcal{S}_K^i + 1) \max_{K' \in \mathcal{S}_K^i} |v_i(\mathbf{x}_{K'})|^2 \leq C \Lambda_m^2 \max_{K' \in \mathcal{S}_K^i} |v_i(\mathbf{x}_{K'})|^2, \end{aligned}$$

which gives the estimate (11) and completes the proof. \square

From the stability property (11), it is formal to obtain the approximation estimate [37, Theorem 3.3].

Theorem 1. *For $i = 0, 1$, there holds*

$$(13) \quad \|v_i - \mathcal{R}_K^{m,i} v_i\|_{H^t(K)} \leq C \Lambda_m h_K^{s-t} \|v\|_{H^s(\mathcal{D}_K^i)}, \quad \forall K \in \mathcal{T}_{h,i}, \quad \forall v \in H^s(\Omega),$$

where $0 \leq t \leq s - 1$ and $2 \leq s \leq m + 1$.

It can be seen that the local polynomial $\mathcal{R}_K^{m,i} v_i$ has an optimal convergence rate if Λ_m admits an upper bound independent of h . We show that such a bound exists if we select a wide enough element patch for every element. In [39, 37], we introduce another constant

$$\Theta_{m,K,i} := \max_{p \in \mathcal{P}_m(\mathcal{D}_K^i)} \frac{\max_{\mathbf{x} \in \mathcal{D}_K^i} p(\mathbf{x})}{\max_{K' \in \mathcal{S}_K^i} p(\mathbf{x}_{K'})}, \quad \forall K \in \mathcal{T}_{h,i}, \quad i = 0, 1.$$

From the inverse inequality, we have $\Lambda_{m,K,i} \leq \Theta_{m,K,i} \leq C \Lambda_{m,K,i}$ for any $K \in \mathcal{T}_{h,i}$. We prove that there exists a threshold \mathcal{N}_m depending on m and C_ν , such that under the condition $\#\mathcal{S}_K^i \geq \mathcal{N}_m$ it holds that $\Theta_{m,K,i} \leq 2$. In this case, the depth t_m still depends only on m, C_ν . Consequently, Λ_m has a uniform upper bound independent of the mesh size and how the interface cuts the background

mesh. However, this theoretical threshold \mathcal{N}_m is usually too large and impractical in the computer implementation. From the definition (10), the constant $\Lambda_{m,K,i}$ equals to the minimum singular value of a local matrix for K , which can be easily obtained. More details and some numerical tests are provided in Appendix A. In the computer implementation, the constant $\Lambda_{m,K,i}$ can serve as an indicator to show whether the patch \mathcal{S}_K^i is large enough.

To close this section, we combine two operators $\mathcal{R}^{m,0}$ and $\mathcal{R}^{m,1}$ to introduce a global operator \mathcal{R}^m and its corresponding space U_h^m on the whole domain Ω . Let χ_i be the characteristic function to Ω_i , and we let $V_h := V_{h,0} \cdot \chi_0 + V_{h,1} \cdot \chi_1$. We define the linear operator \mathcal{R}^m by $\mathcal{R}^m v_h := \mathcal{R}^{m,0} v_{h,0} + \mathcal{R}^{m,1} v_{h,1}$ for any $v_h \in V_h$ with the decomposition $v_h = v_{h,0} \cdot \chi_0 + v_{h,1} \cdot \chi_1$, and let $U_h^m := \mathcal{R}^m V_h$ be its image space. Equivalently, U_h^m can be written as $U_h^m = U_{h,0}^m \cdot \chi_0 + U_{h,1}^m \cdot \chi_1$. Because any $w_h \in U_h^m$ has a unique decomposition $w_h = w_{h,0} \cdot \chi_0 + w_{h,1} \cdot \chi_1$ with $w_{h,i} \in U_{h,i}^m$, we formally introduce two projection operators $(\cdot)^{\pi_i}$ ($i = 0, 1$) such that $w_h^{\pi_i} := w_{h,i} \in U_{h,i}^m$ for any $w_h \in U_h^m$. For any $v \in H^s(\Omega_0 \cup \Omega_1)$, by the Sobolev extension (4) $v_i := v|_{\Omega_i}$ can be extended to the whole domain Ω . Naturally, v admits the decomposition $v = v_0 \cdot \chi_0 + v_1 \cdot \chi_1$. We further formally extend the projection operator $(\cdot)^{\pi_i}$ to v by setting $v^{\pi_i} := v_i \in H^s(\Omega)$.

4. NUMERICAL SCHEME

We present the numerical scheme for the elliptic interface problem (1), based on the Nitsche penalty method and the reconstructed space U_h^m . We define the following discrete variational problem to seek the numerical solution $u_h \in U_h^m$:

$$(14) \quad a_h(u_h, v_h) = l_h(v_h), \quad \forall v_h \in U_h^m,$$

where the bilinear form $a_h(\cdot, \cdot)$ is defined as

$$\begin{aligned} a_h(v_h, w_h) &:= \sum_{K \in \mathcal{T}_h} \int_{K^0 \cup K^1} \alpha \nabla v_h \cdot \nabla w_h \, d\mathbf{x} - \sum_{e \in \mathcal{E}_h} \int_{e^0 \cup e^1} (\{\alpha \nabla v_h\} \cdot [w_h] + \{\alpha \nabla w_h\} \cdot [v_h]) \, ds \\ &\quad - \sum_{K \in \mathcal{T}_h^\Gamma} \int_{\Gamma_K} (\{\alpha \nabla v_h\}_w \cdot [w_h] + \{\alpha \nabla w_h\}_w \cdot [v_h]) \, ds + \sum_{K \in \mathcal{T}_h^\Gamma} \int_{\Gamma_K} \frac{\mu \{\alpha\}_w}{h_K} [v_h] \cdot [w_h] \, ds \\ &\quad + \sum_{e \in \mathcal{E}_{h,0}^I} \int_e \frac{\mu \alpha_0}{h_e} [v_h^{\pi_0}] \cdot [w_h^{\pi_0}] \, ds + \sum_{e \in \mathcal{E}_{h,1}^I \cup \mathcal{E}_h^B} \int_e \frac{\mu \alpha_1}{h_e} [v_h^{\pi_1}] \cdot [w_h^{\pi_1}] \, ds, \end{aligned}$$

for any $v_h, w_h \in U_h := U_h^m + H^2(\Omega_0 \cup \Omega_1)$, and $\mu > 0$ is referred as the penalty parameter. The linear form $l_h(\cdot)$ is given as

$$\begin{aligned} l_h(v_h) &:= \sum_{K \in \mathcal{T}_h} \int_{K^0 \cup K^1} f v_h \, d\mathbf{x} - \sum_{e \in \mathcal{E}_h^B} \int_e g \{\alpha \nabla v_h\} \, ds + \sum_{e \in \mathcal{E}_h^B} \int_e \frac{\mu \alpha}{h_e} g v_h \, ds \\ &\quad + \sum_{K \in \mathcal{T}_h^\Gamma} \int_{\Gamma_K} b \{v_h\}_w \, ds - \sum_{K \in \mathcal{T}_h^\Gamma} \int_{\Gamma_K} a \{\alpha \nabla v_h\}_w \, ds + \sum_{K \in \mathcal{T}_h^\Gamma} \int_{\Gamma_K} \frac{\mu \{\alpha\}_w}{h_K} a_{\mathbf{n}_\Gamma} [v_h] \, ds, \end{aligned}$$

for any $v_h \in U_h$.

We begin the error estimation by introducing the following energy norms for any $v_h \in U_h$:

$$\begin{aligned} |v_h|_e^2 &:= \sum_{e \in \mathcal{E}_{h,0}^I} \frac{\alpha_0}{h_e} \|[v_h^{\pi_0}]\|_{L^2(e)}^2 + \sum_{e \in \mathcal{E}_{h,1}^I \cup \mathcal{E}_h^B} \frac{\alpha_1}{h_e} \|[v_h^{\pi_1}]\|_{L^2(e)}^2 + \sum_{K \in \mathcal{T}_h^\Gamma} \frac{\{\alpha\}_w}{h_K} \|[v_h]\|_{L^2(\Gamma_K)}^2, \\ \|v_h\|_{\text{DG}}^2 &:= \sum_{K \in \mathcal{T}_h} \alpha \|\nabla v_h\|_{L^2(K^0 \cup K^1)}^2 + |v_h|_e^2, \end{aligned}$$

$$\begin{aligned} \|v_h\|_{\text{DG}}^2 &:= \|v_h\|_{\text{DG}}^2 + \sum_{e \in \mathcal{E}_h} \frac{h_e}{\alpha} \|\{\alpha \nabla v_h\}\|_{L^2(e^0 \cup e^1)}^2 + \sum_{K \in \mathcal{T}_h^\Gamma} \frac{h_K}{\{\alpha\}_w} \|\{\alpha \nabla v_h\}_w\|_{L^2(\Gamma_K)}^2, \\ \|v_h\|_*^2 &:= \sum_{K \in \mathcal{T}_{h,0}} \alpha_0 \|\nabla v_h^{\pi_0}\|_{L^2(K)}^2 + \sum_{K \in \mathcal{T}_{h,1}} \alpha_1 \|\nabla v_h^{\pi_1}\|_{L^2(K)}^2 + |v_h|_e^2. \end{aligned}$$

We show that the above norms are equivalent over the approximation space U_h^m , which is crucial for the stability near the interface.

Lemma 4. *There exist constants C such that*

$$(15) \quad \|v_h\|_{\text{DG}} \leq \|v_h\|_{\text{DG}} \leq C \|v_h\|_* \leq C \Lambda_m \|v_h\|_{\text{DG}}, \quad \forall v_h \in U_h^m.$$

Proof. We mainly prove the last estimate $\|v_h\|_* \leq C \Lambda_m \|v_h\|_{\text{DG}}$ while others are straightforward by trace estimates. From the definition, it suffices to prove that for both $i = 0, 1$, there holds $\sum_{K \in \mathcal{T}_h^\Gamma} \alpha_i \|\nabla v_h^{\pi_i}\|_{L^2(K)}^2 \leq C \Lambda_m^2 \|v_h\|_{\text{DG}}^2$. Let $w_{h,i} \in V_{h,i}$ such that $\mathcal{R}^{m,i} w_{h,i} = v_h^{\pi_i}$. For any $K \in \mathcal{T}_{h,i}$, we let $v_K^{\pi_i} := \mathcal{R}_K^{m,i} w_{h,i}$. For any $K \in \mathcal{T}_h^\Gamma$, we split the patch \mathcal{S}_K^i into $\mathcal{S}_K^i = \mathcal{S}_K^{i,\Gamma} + \mathcal{S}_K^{i,\circ}$, where $\mathcal{S}_K^{i,\Gamma} \subset \mathcal{T}_h^\Gamma$ and $\mathcal{S}_K^{i,\circ} \subset \mathcal{T}_{h,i}^\circ$ consist of cut elements and interior elements, respectively. We define a set $\tilde{\mathcal{S}}_K^i := \mathcal{S}_K^{i,\circ} \cup \{(K')^{\sigma_i} : K' \in \mathcal{S}_K^{i,\Gamma}\}$ formed by interior elements. Since $w_{h,i}$ is piecewise constant on $\tilde{\mathcal{S}}_K^i$, we let $w_{\min} := \min_{K' \in \tilde{\mathcal{S}}_K^i} w_{h,i}|_{K'}$ and $w_{\max} := \max_{K' \in \tilde{\mathcal{S}}_K^i} w_{h,i}|_{K'}$. We derive that

$$\begin{aligned} \|\nabla v_h^{\pi_i}\|_{L^2(K)}^2 &= \|\nabla(\mathcal{R}^{m,i} w_{h,i} - w_{\min})\|_{L^2(K)}^2 \leq C h_K^{-2} \|\mathcal{R}^{m,i}(w_{h,i} - w_{\min})\|_{L^2(K)}^2 \\ (16) \quad &\leq C \Lambda_{m,K,i}^2 h_K^{d-2} \sum_{K' \in \mathcal{S}_K^i} ((w_{h,i} - w_{\min})(\mathbf{x}_{K'}))^2 \\ &= C \Lambda_{m,K,i}^2 h_K^{d-2} \left(\sum_{K' \in \mathcal{S}_K^{i,\Gamma}} ((w_{h,i} - w_{\min})(\mathbf{x}_{K'}))^2 + \#\mathcal{S}_K^{i,\circ} (w_{\max} - w_{\min})^2 \right). \end{aligned}$$

For any $K' \in \mathcal{S}_K^{i,\Gamma}$, there holds $(w_{h,i} - w_{\min})(\mathbf{x}_{K'}) = (v_{(K')^{\sigma_i}}^{\pi_i} - w_{\min})(\mathbf{x}_{K'})$, and

$$\begin{aligned} \|(v_{(K')^{\sigma_i}}^{\pi_i} - w_{\min})\|_{L^\infty(K')} &\leq C h_K^{-d/2} \|v_{(K')^{\sigma_i}}^{\pi_i} - w_{\min}\|_{L^2(K')} \leq C h_K^{-d/2} \|v_{(K')^{\sigma_i}}^{\pi_i} - w_{\min}\|_{L^2((K')^{\sigma_i})} \\ &\leq C h_K^{-d/2} (\|v_{(K')^{\sigma_i}}^{\pi_i} - w_{h,i}(\mathbf{x}_{(K')^{\sigma_i}})\|_{L^2((K')^{\sigma_i})} + \|w_{h,i}(\mathbf{x}_{(K')^{\sigma_i}}) - w_{\min}\|_{L^2((K')^{\sigma_i})}) \\ &\leq C h_K^{-d/2} \|v_{(K')^{\sigma_i}}^{\pi_i} - v_{(K')^{\sigma_i}}^{\pi_i}(\mathbf{x}_{(K')^{\sigma_i}})\|_{L^2((K')^{\sigma_i})} + C |w_{\max} - w_{\min}| \\ &\leq C h_K^{1-d/2} \|\nabla v_{(K')^{\sigma_i}}^{\pi_i}\|_{L^2((K')^{\sigma_i})} + C |w_{\max} - w_{\min}|. \end{aligned}$$

Then, we bound the term $|w_{\max} - w_{\min}|$. Since $K_{\max}, K_{\min} \in \mathcal{T}_{h,i}^\circ$, there exist a sequence of interior elements K_1, K_2, \dots, K_m ($m = O(t)$), such that $K_1 = K_{\max}, K_m = K_{\min}, K_j$ and K_{j+1} sharing a common face e_j . It can be seen that

$$(17) \quad |w_{\max} - w_{\min}|^2 = |w_{K_1} - w_{K_m}|^2 \leq C t \sum_{j=1}^{m-1} |w_{K_j} - w_{K_{j+1}}|^2.$$

Let \mathbf{x}_{e_j} be any point in e_j , from the constraint of (6), we find that

$$\begin{aligned} |w_{K_j} - w_{K_{j+1}}|^2 &= |v_{K_j}^{\pi_i}(\mathbf{x}_{K_j}) - v_{K_{j+1}}^{\pi_i}(\mathbf{x}_{K_{j+1}})|^2 \\ (18) \quad &\leq C (|v_{K_j}^{\pi_i}(\mathbf{x}_{K_j}) - v_{K_j}^{\pi_i}(\mathbf{x}_{e_j})|^2 + |v_{K_{j+1}}^{\pi_i}(\mathbf{x}_{K_{j+1}}) - v_{K_{j+1}}^{\pi_i}(\mathbf{x}_{e_j})|^2 + |v_{K_j}^{\pi_i}(\mathbf{x}_{e_j}) - v_{K_{j+1}}^{\pi_i}(\mathbf{x}_{e_j})|^2) \\ &\leq C (h_{K_j}^{2-d} \|\nabla v_{K_j}^{\pi_i}\|_{L^2(K_j)}^2 + h_{K_{j+1}}^{2-d} \|\nabla v_{K_{j+1}}^{\pi_i}\|_{L^2(K_{j+1})}^2 + h_{e_j}^{2-d} \|[v_h^{\pi_i}]\|_{L^2(e_j)}^2). \end{aligned}$$

Collecting all above estimates and summing over all cut elements leads to $\sum_{K \in \mathcal{T}_h^\Gamma} \alpha_i \|\nabla v_h^{\pi_i}\|_{L^2(K)}^2 \leq C \Lambda_m \|v_h\|_{\text{DG}}^2$, which completes the proof. \square

From Lemma 4, the bilinear form is shown to be bounded and coercive under the energy norm $\|\cdot\|_{\text{DG}}$.

Lemma 5. *Let $a_h(\cdot, \cdot)$ be defined with a sufficiently large μ , then*

$$(19) \quad a(v_h, w_h) \leq C \|v_h\|_{\text{DG}} \|w_h\|_{\text{DG}}, \quad \forall v_h, w_h \in U_h,$$

$$(20) \quad a(w_h, w_h) \geq C \Lambda_m^{-2} \|w_h\|_{\text{DG}}^2, \quad \forall w_h \in U_h^m.$$

Proof. The boundedness (19) is quite standard by the Cauchy-Schwarz inequality. The coercivity can be obtained following the canonical procedure in the interior penalty discontinuous Galerkin framework, see [39, 27], i.e., there holds

$$a_h(w_h, w_h) \geq \|w_h\|_{\text{DG}}^2 + (\mu - C_0 t^{-1}) |w_h|_e^2 - C_1 t \|w_h\|_{\text{DG}}^2, \quad \forall t > 0.$$

Together with Lemma 4, the estimate (20) is reached by selecting a sufficiently large penalty, which completes the proof. \square

Lemma 6. *Let $u \in H^2(\Omega_0 \cup \Omega_1)$ be the exact solution to (1), and let $u_h \in U_h^m$ be the numerical solution to (14), then*

$$(21) \quad a_h(u - u_h, v_h) = 0, \quad \forall v_h \in U_h^m.$$

Proof. The orthogonality (21) follows from $[u^{\pi_i}]|_e = 0$ for any $e \in \mathcal{E}_{h,i}$, combined with the identity $[ab] = \{a\}_w [b] + [a] \{b\}_w$. \square

Theorem 2. *Let $a_h(\cdot, \cdot)$ be defined with a sufficiently large μ , and let $u \in H^t(\Omega_0 \cup \Omega_1)$ ($t \geq 2$) be the exact solution to (1), and let $u_h \in U_h^m$ be the numerical solution to (14), then*

$$(22) \quad \|u - u_h\|_{\text{DG}} \leq C \Lambda_m^3 h^s \|\alpha^{\frac{1}{2}} u\|_{H^t(\Omega_0 \cup \Omega_1)},$$

$$(23) \quad \|u - u_h\|_{L^2(\Omega)} \leq C \Lambda_m^4 \alpha_{\min}^{-\frac{1}{2}} h^{s+1} \|\alpha^{\frac{1}{2}} u\|_{H^t(\Omega_0 \cup \Omega_1)},$$

where $s = \min(m, t - 1)$.

Proof. From the approximation property (13) and the trace estimate (5), we have that

$$\|u - u_h\|_{\text{DG}} \leq C \Lambda_m h^s \|\alpha^{\frac{1}{2}} u\|_{H^t(\Omega_0 \cup \Omega_1)}.$$

From Lemma 5 and Lemma 6, we conclude that for any $v_h \in U_h^m$, there holds

$$C \Lambda_m^{-2} \|v_h - u_h\|_{\text{DG}}^2 \leq a_h(v_h - u_h, v_h - u_h) = a_h(u - v_h, v_h - u_h) \leq C \|u - v_h\|_{\text{DG}} \|v_h - u_h\|_{\text{DG}},$$

and combining the triangle inequality yields $\|u - u_h\|_{\text{DG}} \leq C \Lambda_m^2 \inf_{v_h \in U_h^m} \|u - v_h\|_{\text{DG}}$, which leads to the estimate (22).

The L^2 estimate follows from the dual argument. Let $\psi \in H^2(\Omega) \cap H_0^1(\Omega)$ be the solution of the problem

$$-\nabla \cdot (\alpha \nabla \psi) = u - u_h, \quad \text{in } \Omega, \quad \psi = 0, \quad \text{on } \partial\Omega,$$

with $\|\alpha \psi\|_{H^2(\Omega)} \leq C \|u - u_h\|_{L^2(\Omega)}$. Let $\psi_I := \mathcal{R}^m \psi$, and we derive that

$$\begin{aligned} \|u - u_h\|_{L^2(\Omega)}^2 &= a_h(\psi, u - u_h) = a_h(\psi - \psi_I, u - u_h) \leq C \|\psi - \psi_I\|_{\text{DG}} \|u - u_h\|_{\text{DG}} \\ &\leq C h^{s+1} \Lambda_m^4 \|\alpha^{\frac{1}{2}} \psi\|_{H^2(\Omega)} \|\alpha^{\frac{1}{2}} u\|_{H^t(\Omega_0 \cup \Omega_1)}, \end{aligned}$$

which completes the proof. \square

5. PRECONDITIONING

In this section, we present the preconditioning method to the final linear system $A_m \mathbf{x} = \mathbf{b}$ arising from the discrete variational form (14). We first estimate the condition number to the matrix A_m , which requires the relationship between the energy norm and the L^2 norm.

Lemma 7. *For $i = 0, 1$, there holds*

$$(24) \quad \begin{aligned} \|\alpha_0^{\frac{1}{2}} v_h^{\pi_0}\|_{L^2(\Omega_{h,0})} + \|\alpha_1^{\frac{1}{2}} v_h^{\pi_1}\|_{L^2(\Omega_{h,1})} &\leq C \|v_h\|_* \\ &\leq Ch^{-1} (\|\alpha_0^{\frac{1}{2}} v_h^{\pi_0}\|_{L^2(\Omega_{h,0})} + \|\alpha_1^{\frac{1}{2}} v_h^{\pi_1}\|_{L^2(\Omega_{h,1})}), \quad \forall v_h \in U_h^m. \end{aligned}$$

Proof. The upper bound in (24) is straightforward, following the inverse estimate and the trace estimate. For the lower bound, we first state that $\|\alpha^{\frac{1}{2}} v_h\|_{L^2(\Omega)} \leq C \|v_h\|_{\text{DG}}$ (see [29, Lemma 7]). Then, it remains to bound the L^2 norms for cut elements. For any $K \in \mathcal{T}_h^\Gamma$ and $i = 0, 1$, there exists a sequence of elements K_1, K_2, \dots, K_m such that $K_j \in \mathcal{T}_{h,i}$, $K_1 = K$, $K_m = K^{\sigma_i}$ and K_j shares a common face e_j with K_{j+1} . We derive that

$$\|v_h^{\pi_i}\|_{L^2(K_j)}^2 \leq C (h_e^{-1} \|[v_h^{\pi_i}]\|_{L^2(e)}^2 + \|\nabla v_h^{\pi_i}\|_{L^2(K_j)}^2 + \|\nabla v_h^{\pi_i}\|_{L^2(K_{j+1})}^2 + \|v_h^{\pi_i}\|_{L^2(K_{j+1})}^2), \quad 1 \leq j \leq M-1.$$

Hence, there holds

$$\|\alpha_i^{\frac{1}{2}} v_h^{\pi_i}\|_{L^2(K)}^2 \leq C (\|\alpha_i^{\frac{1}{2}} v_h^{\pi_i}\|_{L^2(K^{\sigma_i})}^2 + \sum_{j=1}^M \|\alpha_i^{\frac{1}{2}} \nabla v_h^{\pi_i}\|_{L^2(K_j)}^2 + \sum_{j=1}^{M-1} \alpha_i h_{e_j}^{-1} \|[v_h^{\pi_i}]\|_{L^2(e)}^2).$$

Summation over all cut elements yields that $\|\alpha_i^{\frac{1}{2}} v_h^{\pi_i}\|_{L^2(\Omega_h)} \leq C \|v_h\|_*$, which completes the proof. \square

Theorem 3. *There exists a constant C such that*

$$(25) \quad \kappa(A_m) \leq C \Lambda_m^4 \frac{\alpha_{\max}}{\alpha_{\min}} h^{-2}.$$

Proof. Let $\mathbf{v}_i \in \mathbb{R}^{n_{e,i}}$ be the vector corresponding to any piecewise constant function $v_{h,i} \in V_{h,i}$. Let $\mathbf{v} := (\mathbf{v}_0, \mathbf{v}_1) \in V_h$, there holds

$$\frac{\mathbf{v}^T A_m \mathbf{v}}{\mathbf{v}^T \mathbf{v}} = \frac{a_{h,m}(v_h, v_h)}{\|\alpha_0^{\frac{1}{2}} v_h^{\pi_0}\|_{L^2(\Omega_{h,0})}^2 + \|\alpha_1^{\frac{1}{2}} v_h^{\pi_1}\|_{L^2(\Omega_{h,1})}^2} \frac{\|\alpha_0^{\frac{1}{2}} v_h^{\pi_0}\|_{L^2(\Omega_{h,0})}^2 + \|\alpha_1^{\frac{1}{2}} v_h^{\pi_1}\|_{L^2(\Omega_{h,1})}^2}{\mathbf{v}^T \mathbf{v}}, \quad \forall \mathbf{v} \neq \mathbf{0} \in V_h.$$

The first term in the right hand side can be bounded by applying Lemma 5 - 7. For any $K \in \mathcal{T}_{h,i}$, we have that

$$\|v_h^{\pi_i}\|_{L^2(\Omega_{h,i})}^2 = \sum_{K \in \mathcal{T}_{h,i}} \|v_h^{\pi_i}\|_{L^2(K)}^2 \leq \sum_{K \in \mathcal{T}_{h,i}} \Lambda_{m,K,i}^2 h^d \sum_{K' \in \mathcal{S}_K^i} (v_h^{\pi_i})(\mathbf{x}_{K'})^2 \leq h^d \Lambda_m^2 \mathbf{v}^T \mathbf{v},$$

and by the inverse estimate, there holds

$$\mathbf{v}^T \mathbf{v} = \sum_{K \in \mathcal{T}_{h,i}} ((v_h^{\pi_i})(\mathbf{x}_K))^2 \leq \sum_{K \in \mathcal{T}_{h,i}} \|v_h^{\pi_i}\|_{L^\infty(K)}^2 \leq C \sum_{K \in \mathcal{T}_{h,i}} h_K^{-d} \|v_h^{\pi_i}\|_{L^2(K)}^2 \leq Ch^{-d} \|v_h^{\pi_i}\|_{L^2(\Omega_{h,i})}^2.$$

Collecting all above estimates immediately indicates that $C \alpha_{\min} \Lambda_m^{-2} \leq \frac{\mathbf{v}^T A_m \mathbf{v}}{\mathbf{v}^T \mathbf{v}} \leq C \alpha_{\max} \Lambda_m^2 h^{-2}$ for any vector \mathbf{v} , which yields the estimate (25) and completes the proof. \square

From Theorem 3, the resulting matrix has a condition number of $O(h^{-2})$ independent of the interface intersecting the mesh.

In the rest of this section, we present a preconditioning method for the system $A_m \mathbf{x} = \mathbf{b}$. It is noticeable that the reconstructed space U_h^m always has the same dimensions for all $m \geq 0$. This

property inspires us to precondition the high-order scheme by the lowest-order scheme, i.e., $a_h(\cdot, \cdot)$ over the space $V_h \times V_h$. We define the bilinear form $a_{h,0}$ as follow,

$$(26) \quad \begin{aligned} a_{h,0}(v_h, w_h) := & \sum_{e \in \mathcal{E}_{h,0}^I} \frac{\alpha_0}{h_e} \int_e [v_h^{\pi_0}] \cdot [w_h^{\pi_0}] ds + \sum_{e \in \mathcal{E}_{h,1}^I \cup \mathcal{E}_h^B} \frac{\alpha_1}{h_e} \int_e [v_h^{\pi_1}] \cdot [w_h^{\pi_1}] ds \\ & + \sum_{K \in \mathcal{T}_h^\Gamma} \frac{\{\alpha\}_w}{h_K} \int_{\Gamma_K} [v_h] \cdot [w_h] ds, \quad \forall v_h, w_h \in V_h. \end{aligned}$$

Here, $a_{h,0}(v_h, w_h) = a_h(v_h, w_h)$ for $\forall v_h, w_h \in V_h$ with the penalty parameter fixed as $\mu = 1$. Let A_0 be the matrix arising from $a_{h,0}(\cdot, \cdot)$. It can be observed that $a_{h,0}(v_h, v_h) = \|v_h\|_{\text{DG}}^2 = \|v_h\|_*^2$ for $\forall v_h \in V_h$, which immediately indicates A_0 is invertible. We will show that the inverse A_0^{-1} can serve as an optimal preconditioner for A_m for any accuracy $m \geq 1$, which is based on the following equivalence property for the reconstruction operator \mathcal{R}^m under the energy norm.

Lemma 8. *There exist constants C such that*

$$(27) \quad \|v_h\|_* \leq C \|\mathcal{R}^m v_h\|_* \leq C \Lambda_m \|v_h\|_*, \quad \forall v_h \in V_h.$$

Proof. We first verify the lower bound in (27). For any face $e \in \mathcal{E}_{h,0}^I$ shared by two elements K_- and K_+ , the jump $[v_h^{\pi_0}]|_e$ can be bounded as (18), that is

$$\alpha_0 h_e^{-1} \|[v_h^{\pi_0}]\|_{L^2(e)}^2 \leq C \alpha_0 (\|\nabla \mathcal{R}^{m,0} v_h^{\pi_0}\|_{L^2(K_-)}^2 + \|\nabla \mathcal{R}^{m,0} v_h^{\pi_0}\|_{L^2(K_+)}^2 + h_e^{-1} \|\mathcal{R}^{m,0} v_h^{\pi_0}\|_{L^2(e)}^2).$$

A similar estimate can be established for faces $e \in \mathcal{E}_{h,1}^I \cup \mathcal{E}_h^B$. For any cut element $K \in \mathcal{T}_h^\Gamma$, we derive that

$$\begin{aligned} \{\alpha\}_w h_K^{-1} \|[v_h]\|_{L^2(\Gamma_K)}^2 & \leq C \{\alpha\}_w h_K^{-1} (\|[v_h - \mathcal{R}^m v_h]\|_{L^2(\Gamma_K)}^2 + \|\mathcal{R}^m v_h\|_{L^2(\Gamma_K)}^2), \\ & \leq C h_K^{-1} (\alpha_0 \|v_h^{\pi_0} - \mathcal{R}_K^{m,0} v_h^{\pi_0}\|_{L^2(\Gamma_K)}^2 + \alpha_1 \|v_h^{\pi_1} - \mathcal{R}_K^{m,1} v_h^{\pi_1}\|_{L^2(\Gamma_K)}^2 + \{\alpha\}_w \|\mathcal{R}^m v_h\|_{L^2(\Gamma_K)}^2). \end{aligned}$$

For $i = 0, 1$, together with the constraint in (6) that $\mathcal{R}_K^{m,i} v_h^{\pi_i}(\mathbf{x}_K) = v_h^{\pi_i}(\mathbf{x}_K)$, there holds

$$\alpha_i h_K^{-1} \|v_h^{\pi_i} - \mathcal{R}_K^{m,i} v_h^{\pi_i}\|_{L^2(\Gamma_K)}^2 \leq C \alpha_i h_K^{d-2} \|\mathcal{R}_K^{m,i} v_h^{\pi_i} - \mathcal{R}_K^{m,i} v_h^{\pi_i}(\mathbf{x}_K)\|_{L^\infty(K)}^2 \leq C \alpha_i \|\nabla \mathcal{R}_K^{m,i} v_h^{\pi_i}\|_{L^2(K)}^2.$$

Collecting all estimates yields the lower bound in (27).

We next turn to the upper bound of (27). For the trace term $\|\mathcal{R}^{m,0} v_h^{\pi_0}\|_{L^2(e)}$ on $e \in \mathcal{E}_{h,0}^I$, we let e be shared by elements K_+ and K_- and derive that

$$\alpha_0 h_e^{-1} \|\mathcal{R}^{m,0} v_h^{\pi_0}\|_{L^2(e)}^2 \leq C \alpha_0 h_e^{-1} (\|[v_h^{\pi_0}]\|_{L^2(e)}^2 + \|\mathcal{R}^{m,0} v_h^{\pi_0} - v_h^{\pi_0}\|_{L^2(e)}^2).$$

From the constraint in (6), the second term can be bounded by

$$\begin{aligned} h_e^{-1} \|\mathcal{R}^{m,0} v_h^{\pi_0} - v_h^{\pi_0}\|_{L^2(e)}^2 & \leq C h_e^{-1} (\|\mathcal{R}_{K_-}^{m,0} v_h^{\pi_0} - v_h^{\pi_0}(\mathbf{x}_{K_-})\|_{L^2(e)}^2 + \|\mathcal{R}_{K_+}^{m,0} v_h^{\pi_0} - v_h^{\pi_0}(\mathbf{x}_{K_+})\|_{L^2(e)}^2) \\ & \leq C (\|\nabla \mathcal{R}_{K_-}^{m,0} v_h^{\pi_0}\|_{L^2(K_-)}^2 + \|\nabla \mathcal{R}_{K_+}^{m,0} v_h^{\pi_0}\|_{L^2(K_+)}^2). \end{aligned}$$

Analogously, the trace $\|\mathcal{R}^{m,1} v_h^{\pi_1}\|_{L^2(e)}$ on $e \in \mathcal{E}_{h,1}^I \cup \mathcal{E}_h^B$ can be estimated by the same procedure. For cut elements, there holds

$$\begin{aligned} \{\alpha\}_w h_K^{-1} \|\mathcal{R}^{m,i} v_h\|_{L^2(\Gamma_K)}^2 & \leq C h_K^{-1} (\{\alpha\}_w \|[v_h - \mathcal{R}^{m,i} v_h]\|_{L^2(\Gamma_K)}^2 + \{\alpha\}_w \|[v_h]\|_{L^2(\Gamma_K)}^2) \\ & \leq C h_K^{-1} (\alpha_0 \|\mathcal{R}_K^{m,0} v_h^{\pi_0} - v_h^{\pi_0}(\mathbf{x}_K)\|_{L^2(\Gamma_K)}^2 + \alpha_1 \|\mathcal{R}_K^{m,1} v_h^{\pi_1} - v_h^{\pi_1}(\mathbf{x}_K)\|_{L^2(\Gamma_K)}^2 + \{\alpha\}_w \|[v_h]\|_{L^2(\Gamma_K)}^2). \end{aligned}$$

Combining above estimates leads to

$$\|\mathcal{R}^m v_h\|_*^2 \leq C \left(\sum_{K \in \mathcal{T}_{h,0}} \alpha_0 \|\nabla \mathcal{R}_K^{m,0} v_h^{\pi_0}\|_{L^2(K)}^2 + \sum_{K \in \mathcal{T}_{h,1}} \alpha_1 \|\nabla \mathcal{R}_K^{m,1} v_h^{\pi_1}\|_{L^2(K)}^2 \right) + C \|v_h\|_*^2.$$

It remains to bound the L^2 norm for the gradient. For any $K \in \mathcal{T}_{h,i}$, we let $v_{\min} := \min_{K' \in \mathcal{S}_K^i}(v_h^{\pi_i}|_{K'})$ and $v_{\max} := \max_{K' \in \mathcal{S}_K^i}(v_h^{\pi_i}|_{K'})$. As (16), we find that

$$\|\nabla \mathcal{R}_K^{m,i} v_h^{\pi_i}\|_{L^2(K)}^2 \leq C \Lambda_{m,K,i}^2 \# \mathcal{S}_K^i (v_{\max} - v_{\min})^2,$$

and by (17) - (18), there holds

$$\sum_{K \in \mathcal{T}_{h,i}} \alpha_i \|\nabla \mathcal{R}_K^{m,i} v_h^{\pi_i}\|_{L^2(K)}^2 \leq C \Lambda_m^2 \sum_{e \in \mathcal{E}_{h,i}^I} \alpha_i h_e^{-1} \|[v_h^{\pi_i}]\|_{L^2(e)}^2 \leq C \Lambda_m^2 \|v_h\|_*^2,$$

which leads to the desired estimate (27) and completes the proof. \square

A direct consequence of (27) is the following estimate to the preconditioned system.

Theorem 4. *There exists a constant C such that*

$$(28) \quad \kappa(A_0^{-1} A_m) \leq C \Lambda_m^4.$$

Proof. From (19), (20) and (27), we deduce that

$$\begin{aligned} a_0(v_h, v_h) &= \|v_h\|_*^2 \leq \|\mathcal{R}^m v_h\|_*^2 \leq C \Lambda_m^2 a_h(\mathcal{R}^m v_h, \mathcal{R}^m v_h) \\ &\leq C \Lambda_m^2 \|\mathcal{R}^m v_h\|_*^2 \leq C \Lambda_m^4 \|v_h\|_*^2 = a_0(v_h, v_h), \quad \forall v_h \in V_h, \end{aligned}$$

which brings (28) and completes the proof. \square

Theorem 4 the resulting linear system can be solved by using the Krylov iterative method (e.g. CG and GMRES) with A_0^{-1} as the preconditioner. In addition, this preconditioner is robust to the coefficient. Generally speaking, in the iterative steps, the matrix-vector product $\mathbf{y} = A_0^{-1} \mathbf{z}$ is computed by solving the linear system $A_0 \mathbf{y} = \mathbf{z}$. Although A_0 arises from the lowest-order scheme, it still has a condition number of $O(h^{-2})$ as Theorem 3. The second part in our preconditioning method is to give a fast solver as an approximation to the inverse A_0^{-1} . We will follow the multigrid idea of the smoothed aggregation method [48, 49].

Assume that the mesh \mathcal{T}_h is obtained by successively refining a coarse (unfitted) mesh \mathcal{T}_{h_0} for several times, i.e., there exist a series of meshes $\mathcal{T}_{h_0}, \mathcal{T}_{h_1}, \dots, \mathcal{T}_{h_J}$ such that $\mathcal{T}_{h_J} = \mathcal{T}_h$ and $\mathcal{T}_{h_{j+1}}$ is obtained by globally refining the mesh \mathcal{T}_{h_j} , and thus $h_j = 2^{-j} h_0$ and $h_J = h$. For \mathcal{T}_{h_j} , we let $\mathcal{T}_{h_j,i}$ ($i = 0, 1$), $\Omega_{h_j,i}$ be the same as in Section 2, and we let $V_{h_j,i}$ be the piecewise constant space on $\mathcal{T}_{h_j,i}$. Note that $V_{h_j,i}$ is defined on the domain $\Omega_{h_j,i}$, and there holds $\Omega_{h_j,i} \subset \Omega_{h_k,i}$ for any $j \geq k$, which further implies $V_{h_k,i} \subset V_{h_j,i}$. From this fact, we introduce an operator operator $I_{k,j}^i$ ($j \geq k$): $V_{h_k,i} \rightarrow V_{h_j,i}$ such that $I_{k,j}^i v_{h_k,i} := v_{h_k,i}|_{\Omega_{h_k,i}}$ for $\forall v_{h_k,i} \in V_{h_k,i}$. We define an inner product $(\cdot, \cdot)_{\alpha,2}$ as

$$(v, w)_{\alpha,2} := (\alpha_0 v, w)_{L^2(\Omega_0)} + (\alpha_1 v, w)_{L^2(\Omega_1)}, \quad \forall v, w \in L^2(\Omega),$$

with the induced norm $\|\cdot\|_{\alpha,2}$. Moreover, we introduce the prolongation operator $I_{j,k}^i$ ($j \geq k$): $V_{h_j,i} \rightarrow V_{h_k,i}$ such that $I_{j,k}^i v_{h_j,i}$ is the projection of $v_{h_j,i}$ into $V_{h_k,i}$ under the norm $\|\cdot\|_{\alpha,2}$ for $\forall v_{h_j,i} \in V_{h_j,i}$. Then, we have that $(I_{k,j}^i)^T = I_{j,k}^i$ under the inner product $(\cdot, \cdot)_{\alpha,2}$. We define a global space $V_{h_j} := V_{h_j,0} \cdot \chi_0 + V_{h_j,1} \cdot \chi_1$ by concatenating spaces $V_{h_j,0}$ and $V_{h_j,1}$, and define the operator $I_{j,k} := I_{j,k}^0 \cdot \chi_0 + I_{j,k}^1 \cdot \chi_1$.

To present the multigrid method, we introduce a linear operator $\mathcal{A}: V_{h_J} \rightarrow V_{h_J}$ on the finest level J by

$$(\mathcal{A}v_h, w_h)_{\alpha,2} = a_{h,0}(v_h, w_h), \quad \forall v_h, w_h \in V_{h_J},$$

with the induced norm $\|v_h\|_{\mathcal{A}}^2 = (\mathcal{A}v_h, v_h)_{\alpha,2}$. On each level $j \leq J$, we define the operator \mathcal{A}_j and the symmetric prolongator smoother S_j in a recursive manner, which read

$$(29) \quad \mathcal{A}_j := (S_{j+1} I_{j,j+1})^T \mathcal{A}_{j+1} S_{j+1} I_{j,j+1}, \quad S_j := I - (\lambda_j)^{-1} \mathcal{A}_j, \quad \mathcal{A}_J := \mathcal{A},$$

where λ_j is a parameter will be specified later. For any linear operator, we let $\sigma(\cdot)$ and $\rho(\cdot)$ be its spectrum and its largest eigenvalue, respectively. We will show that λ_j can be chosen as

$$(30) \quad \lambda_j = 4^{j-J}\lambda, \quad \lambda > \rho(\mathcal{A}),$$

and serve as a bound of $\rho(\mathcal{A}_j)$. From Theorem 3, the parameter λ can be selected as $\lambda = O(h^{-2})$. By (29), we present a \mathcal{W} -cycle multigrid algorithm in Algorithm 1. From (29), the operator \mathcal{A}_j can be rewritten into the form $\mathcal{A}_j = Q_j^T \mathcal{A}_J Q_j$, where $Q_j : V_{h_j} \rightarrow V_{h_J}$ is defined by

$$Q_j = S_J I_{J-1, J} S_{J-1} I_{J-2, J-1} \dots S_{j+1} I_{j, j+1}, \quad 1 \leq j \leq J-1, \quad Q_J = I.$$

By [48], the convergence analysis to Algorithm 1 is established on the following results.

The first is the weak approximation property of the space V_{h_j} .

Lemma 9. *There exists a constant C such that*

$$(31) \quad \min_{w_{h_j} \in V_{h_j}} \|v_h - w_{h_j}\|_{\alpha, 2}^2 \leq C 4^{J-j} h^2 \|v_h\|_{\mathcal{A}}^2, \quad \forall v_h \in V_{h_J}, \quad 1 \leq j \leq J.$$

Proof. By [30, Theorem 2.1], for $v_h^{\pi_i} \in V_{h_J, i}$, there exists a function $v_{h, i} \in H^1(\Omega_{h_J, i})$ such that

$$\sum_{K \in \mathcal{T}_{h, i}} \alpha_i h_K^{2q-2} |v_h^{\pi_i} - v_{h, i}|_{H^q(K)}^2 \leq C \sum_{e \in \mathcal{E}_{h, i}^I} \alpha_i h_e^{-1} \| [v_h^{\pi_i}] \|_{L^2(e)}^2 \leq C \|v_h\|_*^2, \quad \forall q = 0, 1.$$

Since $v_h^{\pi_i}$ is piecewise constant on \mathcal{T}_h , we find that $\alpha_i |v_{h, i}|_{H^1(\Omega_i)}^2 \leq \alpha_i |v_{h, i}|_{H^1(\Omega_{h_J, i})}^2 \leq C \|v_h\|_{\mathcal{A}}^2$. From Lemma 7, there holds $\alpha_i \|v_{h, i}\|_{L^2(\Omega_i)}^2 \leq C \|v_h\|_{\mathcal{A}}^2$. Let v_i be the Sobolev extension of $v_{h, i}|_{\Omega_i}$ to Ω , which satisfy that $v_i|_{\Omega_i} = v_{h, i}$ and $\alpha_i \|v_i\|_{H^1(\Omega)}^2 \leq C \alpha_i \|v_{h, i}\|_{H^1(\Omega_i)}^2 \leq C \|v_h\|_{\mathcal{A}}^2$. Let $w_{h_j, i}$ be the L^2 interpolant of v_i into the space $V_{h_j, i}$ such that $\|w_{h_j, i} - v_i\|_{L^2(\Omega_{h_j, i})} \leq Ch_j \|v_i\|_{H^1(\Omega)}$. We derive that

$$\begin{aligned} \|v_h - w_{h_j}\|_{\alpha, 2}^2 &= \sum_{i=0,1} \alpha_i \|v_h^{\pi_i} - w_{h_j, i}\|_{L^2(\Omega_i)}^2 \\ &\leq C \sum_{i=0,1} \alpha_i (\|v_i - w_{h_j, i}\|_{L^2(\Omega_i)}^2 + \|v_i - v_h^{\pi_i}\|_{L^2(\Omega_i)}^2) \leq Ch_j^2 \|v_h\|_{\mathcal{A}}^2, \end{aligned}$$

which leads to (31) and completes the proof. \square

Next, we demonstrate that the selection (30) is suitable.

Lemma 10. *Let λ_j be taken as (30), there holds*

$$(32) \quad \rho(\mathcal{A}_j) \leq \rho(S_{j+1}^T \mathcal{A}_{j+1} S_{j+1}) < 4^{j-J}\lambda = \lambda_j, \quad 1 \leq j \leq J-1.$$

Proof. We prove the estimate (32) for the finest level $j = J-1$. In this case, S_{j+1} has the form $S_J = I - \mathcal{A}_J$. By the definition of $\mathcal{A}_j = \mathcal{A}_{J-1}$, we deduce that

$$\begin{aligned} \rho(\mathcal{A}_{J-1}) &= \max_{v_{h_j} \in V_{h_j}} \frac{(Q_j v_{h_j}, \mathcal{A}_J(Q_j v_{h_j}))_{\alpha, 2}}{(v_{h_j}, v_{h_j})_{\alpha, 2}} = \max_{v_{h_j} \in V_{h_j}} \frac{(I_{j, J} v_{h_j}, (S_J^T \mathcal{A}_J S_J)(I_{j, J} v_{h_j}))_{\alpha, 2}}{(I_{j, J} v_{h_j}, I_{j, J} v_{h_j})_{\alpha, 2}} \\ &\leq \max_{v_{h_J} \in V_J} \frac{(v_{h_J}, (S_J^T \mathcal{A}_J S_J) v_{h_J})_{\alpha, 2}}{(v_{h_J}, v_{h_J})_{\alpha, 2}} \leq \rho(S_J^T \mathcal{A}_J S_J). \end{aligned}$$

Since $\lambda_J = \lambda > \rho(\mathcal{A}_J)$, we know that $\rho(\mathcal{A}_J/\lambda_J) < 1$. By the direct calculation, we obtain

$$S_J^T \mathcal{A}_J S_J = (I - \mathcal{A}_J)^2 \mathcal{A}_J,$$

and

$$\rho(S_J^T \mathcal{A}_J S_J) = \lambda_J \max_{t \in \sigma(\lambda_J^{-1} \mathcal{A}_J)} (1-t)^2 t \leq \lambda_J \max_{t \in (0,1)} (1-t)^2 t < 4^{-1} \lambda,$$

Algorithm 1: \mathcal{W} -cycle Multigrid Solver, MGSolverI($\mathbf{y}_j, \mathbf{z}_j, j$)**Input:** the initial guess \mathbf{y}_j , the right hand side \mathbf{z}_j , the level j ;**Output:** the solution \mathbf{y}_j ;**if** $j = 1$ **then** $\mathcal{A}_1 \mathbf{y}_1 = \mathbf{z}_1$ is solved by the direct method. return \mathbf{y}_1 ;**if** $j > 1$ **then** pre-smoothing: apply Gauss-Seidel sweep on $\mathcal{A}_j \mathbf{y}_j = \mathbf{z}_j$; correction on coarse mesh: set $\boldsymbol{\xi} = (S_j I_{j-1}^j)^T (\mathbf{z}_j - \mathcal{A}_j \mathbf{y}_j)$; let $\mathbf{w}_1 = \mathbf{0}$, and update \mathbf{w}_1 by MGSolverI($\mathbf{w}_1, \boldsymbol{\xi}, j-1$); set $\mathbf{w}_2 = \text{MGSolverI}(\mathbf{w}_1, \boldsymbol{\xi}, j-1)$; set $\mathbf{y}_j = \mathbf{y}_j + S_j I_{j-1}^j \mathbf{w}_2$; post-smoothing: apply Gauss-Seidel sweep on $\mathcal{A}_j \mathbf{y}_j = \mathbf{z}_j$; return \mathbf{y}_j ;

which gives the estimate (32) for $j = J-1$ and indicates $\varrho(\mathcal{A}_{J-1}) \leq \lambda_{J-1}$. The last inequality follows from the fact that the maximum value of the function $f(t) = (1-t)^2 t$ on $(0, 1)$ is reached at $t_0 = 3^{-1}$, and $f(t) \leq f(t_0) < 4^{-1}$ for any $t \in (0, 1)$. By the same procedure, we conclude the estimate (32) at level $j-1$ from the result at j , which completes the proof. \square

Combining the estimate (32) and the definition of S_j , we have that

$$(33) \quad \rho(S_j) = \max_{t \in \sigma(\lambda_j^{-1} \mathcal{A}_j)} (1-t) < 1, \quad \sigma(S_j) \subset (0, 1), \quad 1 \leq j \leq J.$$

Then, both S_j and \mathcal{A}_j are symmetric and positive definite. From \mathcal{A}_j , we introduce an induced norm $\|v_{h_j}\|_{\mathcal{A}_j}^2 := (v_{h_j}, \mathcal{A}_j v_{h_j})_{\alpha, 2}$ for $\forall v_{h_j} \in V_{h_j}$. We further derive that

$$(34) \quad \|v_{h_j} - S_j v_{h_j}\|_{\alpha, 2} = \|\lambda_j^{-1} \mathcal{A}_j v_{h_j}\|_{\alpha, 2} \leq \lambda_j^{-1/2} \|v_{h_j}\|_{\mathcal{A}_j} \leq \frac{1}{\sqrt{\rho(\mathcal{A}_j)}} \|v_{h_j}\|_{\mathcal{A}_j}, \quad \forall v_{h_j} \in V_{h_j}.$$

Let $\tilde{Q}_j := Q_j I_j^j$ on the space V_h , we have the following results.

Lemma 11. *There exist constants C_0, C_1 such that*

$$(35) \quad \|\tilde{Q}_j v_h\|_{\mathcal{A}} \leq \tilde{C}(j) \|v_h\|_{\mathcal{A}}, \quad \forall v_h \in V_h, \quad 1 \leq j \leq J,$$

where $\tilde{C}(j) = C_0 + C_1 j$, and there exist constants C_2, C_3 such that

$$(36) \quad \|(\tilde{Q}_j - \tilde{Q}_{j+1}) v_h\|_{\alpha, 2} \leq \frac{\hat{C}(j)}{\sqrt{\rho(\mathcal{A}_{j+1})}} \|v_h\|_{\mathcal{A}}, \quad \forall v_h \in V_h, \quad 1 \leq j \leq J-1,$$

where $\hat{C}(j) = C_2 + C_3 j$.

Proof. For the first estimate (35), we deduce that

$$(37) \quad \begin{aligned} \|\tilde{Q}_j v_h\|_{\mathcal{A}} &= \|Q_j I_j^j v_h\|_{\mathcal{A}} = \|Q_{j+1} S_{j+1} I_j^{j+1} I_j^j v_h\|_{\mathcal{A}} = \|S_{j+1} I_j^{j+1} I_j^j v_h\|_{\mathcal{A}_{j+1}} \\ &\leq \|S_{j+1} I_j^{j+1} v_h\|_{\mathcal{A}_{j+1}} + \|S_{j+1} (I_j^{j+1} - I_j^j) v_h\|_{\mathcal{A}_{j+1}}. \end{aligned}$$

By (33), we have that $\|S_{j+1} I_j^{j+1} v_h\|_{\mathcal{A}_{j+1}} \leq \|I_j^{j+1} v_h\|_{\mathcal{A}_{j+1}} = \|\tilde{Q}_{j+1} v_h\|_{\mathcal{A}}$. From the weak approximation property (31) and (32), it can be seen that

$$(38) \quad \begin{aligned} \|S_{j+1} (I_j^{j+1} - I_j^j) v_h\|_{\mathcal{A}_{j+1}}^2 &= ((I_j^{j+1} - I_j^j) v_h, S_{j+1}^T \mathcal{A}_{j+1} S_{j+1} (I_j^{j+1} - I_j^j) v_h)_{\alpha, 2} \\ &\leq 4^{j-J} \lambda \|I_j^{j+1} (v_h - I_j^j v_h)\|_{\alpha, 2}^2 \leq 4^{j-J} \lambda \|v_h - I_j^j v_h\|_{\alpha, 2}^2 \leq C \|v_h\|_{\mathcal{A}}^2. \end{aligned}$$

Combining (37) - (38) directly leads to the desired estimate (35).

For the second estimate (36), we have that

$$\begin{aligned} \|(\tilde{Q}_j - \tilde{Q}_{j+1})v_h\|_{\alpha,2} &= \|Q_{j+1}(S_{j+1}I_j^{j+1}I_j^j - I_j^{j+1})v_h\|_{\alpha,2} \leq \|(S_{j+1}I_j^{j+1}I_j^j - I_j^{j+1})v_h\|_{\alpha,2} \\ &\leq \|S_{j+1}(I_j^{j+1}I_j^j - I_j^{j+1})v_h\|_{\alpha,2} + \|(I_j^{j+1} - S_{j+1}I_j^{j+1})v_h\|_{\alpha,2}. \end{aligned}$$

The first term can be bounded by the weak approximation property (31) and (33), i.e.

$$\|S_{j+1}(I_j^{j+1}I_j^j - I_j^{j+1})v_h\|_{\alpha,2} \leq \|I_j^{j+1}(I_j^j v_h - v_h)\|_{\alpha,2} \leq \|v_h - I_j^j v_h\|_{\alpha,2} \leq \frac{C}{\sqrt{\rho(\mathcal{A}_{j+1})}} \|v_h\|_{\mathcal{A}}.$$

The second term can be estimated by (34), which reads

$$\begin{aligned} \|I_j^{j+1}v_h - S_{j+1}I_j^{j+1}v_h\|_{\alpha,2} &\leq \frac{C}{\sqrt{\rho(\mathcal{A}_{j+1})}} \|I_j^{j+1}v_h\|_{\mathcal{A}_{j+1}} = \frac{C}{\sqrt{\rho(\mathcal{A}_{j+1})}} \|Q_{j+1}I_j^{j+1}v_h\|_{\mathcal{A}} \\ &= \frac{C}{\sqrt{\rho(\mathcal{A}_{j+1})}} \|\tilde{Q}_{j+1}v_h\|_{\mathcal{A}} \leq \frac{C\tilde{C}(j)}{\sqrt{\rho(\mathcal{A}_{j+1})}} \|v_h\|_{\mathcal{A}}. \end{aligned}$$

The above two estimates lead to the estimate (36), which completes the proof. \square

From [48, Theorem 3.5], Lemma 11 gives the convergence rate of Algorithm 1.

Theorem 5. *For the linear system $A_0\mathbf{y} = \mathbf{z}$, there holds*

$$(39) \quad \|\mathbf{y} - \text{MG}(\tilde{\mathbf{y}}, \mathbf{z})\|_{\mathcal{A}} \leq (1 - \frac{1}{C(J)}) \|\mathbf{y} - \tilde{\mathbf{y}}\|_{\mathcal{A}}, \quad C(J) = O(J^3).$$

As a result, the linear system $A_m\mathbf{x} = \mathbf{b}$ of (14) can be solved by the CG method using Algorithm 1 as the preconditioner.

Finally, we present another \mathcal{W} -cycle multigrid algorithm in Algorithm 2 for the system $A_0\mathbf{y} = \mathbf{z}$, which is simpler than Algorithm 1 and is more close to the standard geometrical multigrid. In Algorithm 2, the smoother S_j is replaced by the identical operator. On each level j , we define a bilinear form

$$\begin{aligned} a_{h_j,0}(v_{h_j}, w_{h_j}) &:= \sum_{e \in \mathcal{E}_{h_j,0}^I} \frac{\alpha_0}{h_e} \int_e [v_{h_j}^{\pi_0}] \cdot [w_{h_j}^{\pi_0}] ds + \sum_{e \in \mathcal{E}_{h_j,1}^I \cup \mathcal{E}_{h_j}^B} \frac{\alpha_1}{h_e} \int_e [v_{h_j}^{\pi_1}] \cdot [w_{h_j}^{\pi_1}] ds \\ &+ \sum_{K \in \mathcal{T}_{h_j}^\Gamma} \frac{\{\alpha\}_w}{h_K} \int_{\Gamma_K} [v_{h_j}] \cdot [w_{h_j}] ds, \quad \forall v_{h_j}, w_{h_j} \in V_{h_j}, \end{aligned}$$

which is the interior penalty scheme on \mathcal{T}_{h_j} over piecewise constant spaces $V_{h_j} \times V_{h_j}$. Let $A_{0,j}$ be the matrix of $a_{h_j,0}(\cdot, \cdot)$, and in Algorithm 2, we consider the linear system of the matrix $A_{0,j}$ on each level. As a numerical observation, the iterative solver still works well with choosing Algorithm 2 as the preconditioner. The convergence study is currently left as a future topic.

6. NUMERICAL RESULTS

In this section, we carry out a series of numerical tests to demonstrate the numerical performance of the proposed method and the efficiency of the preconditioner. For all examples, the data functions f , g and the jump functions a and b are chosen from the exact solution. The interfaces in tests are described by level set functions. In the numerical scheme, the quadrature rule of the integration on curved domains as

$$\int_{K^0} f d\mathbf{x}, \quad \int_{K^1} f d\mathbf{x}, \quad \int_{\Gamma_K} f ds, \quad \forall K \in \mathcal{T}_h^\Gamma,$$

Algorithm 2: \mathcal{W} -cycle Multigrid Solver, $\text{MGSolverII}(\mathbf{y}_j, \mathbf{z}_j, j)$

Input: the initial guess \mathbf{y}_j , the right hand side \mathbf{z}_j , the level j ;

Output: the solution \mathbf{y}_j ;

if $j = 1$ **then**

$A_{\mathcal{L},1}\mathbf{y}_1 = \mathbf{z}_1$ is solved by the direct method.
 return \mathbf{x}_1 ;

if $j > 1$ **then**

 pre-smoothing: apply Gauss-Seidel sweep on $A_{\mathcal{L},j}\mathbf{y}_j = \mathbf{z}_j$;
 correction on coarse mesh: set $\boldsymbol{\xi} = I_j^{j-1}(\mathbf{z}_j - A_{\mathcal{L},j}\mathbf{y}_j)$;
 let $\mathbf{w}_1 = \mathbf{0}$, and update \mathbf{w}_1 by $\text{MGSolverII}(\mathbf{w}_1, \boldsymbol{\xi}, j-1)$;
 set $\mathbf{w}_2 = \text{MGSolverII}(\mathbf{w}_1, \boldsymbol{\xi}, j-1)$;
 set $\mathbf{y}_j = \mathbf{y}_j + I_{j-1}^j \mathbf{w}_2$;
 post-smoothing: apply Gauss-Seidel sweep on $A_{\mathcal{L},j}\mathbf{y}_j = \mathbf{z}_j$;
 return \mathbf{y}_j ;

are required. We refer to [17] for the method that generates quadrature points and weights for such integrals, and the subroutines are freely available online. In two dimensions, the computational domain Ω is fixed as the square domain $\Omega = (-1, 1)^2$, and we adopt a family of triangular meshes with $h = 1/10, \dots, 1/80$ for all tests, see Fig. 1. In three dimensions, the domain Ω is taken to be the cube $\Omega = (0, 1)^3$, and we solve the test on tetrahedral meshes with $h = 1/8, \dots, 1/64$, see Fig. 2.

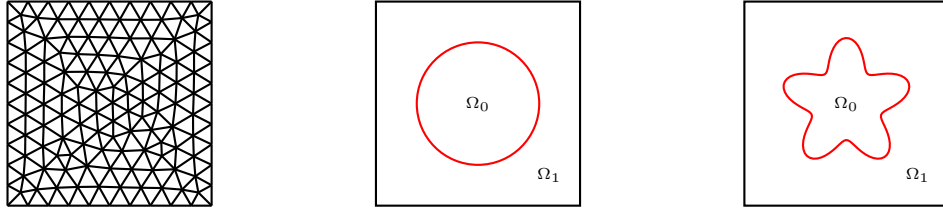


FIGURE 1. The unfitted mesh and the interfaces in two dimensions.

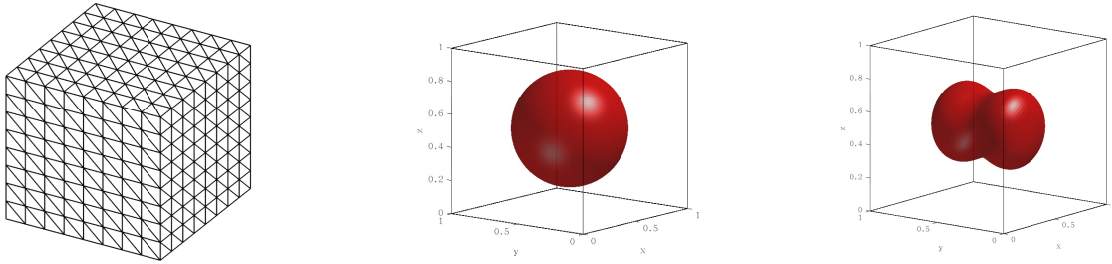


FIGURE 2. The unfitted mesh and the interfaces in three dimensions.

Example 1. In the first example, we solve an interface problem with a circular interface centered at the origin with the radius $r = 0.6$, see Fig. 1. The exact solution and the coefficient are given by

$$u(x, y) = \begin{cases} \sin(\pi x) \sin(\pi y), & \text{in } \Omega_0, \\ \cos(2\pi x) \cos(4\pi y), & \text{in } \Omega_1, \end{cases} \quad \alpha = \begin{cases} \alpha_0, & \text{in } \Omega_0, \\ 1, & \text{in } \Omega_1. \end{cases}$$

The numerical errors for $\alpha_0 = 10$ are displayed in Fig. 3. It can be observed that the errors under both the energy norm and the L^2 norm converge to zero at the optimal rate $O(h^m)$ and $O(h^{m+1})$, respectively, which confirm the theoretical preconditions given in Theorem 2.

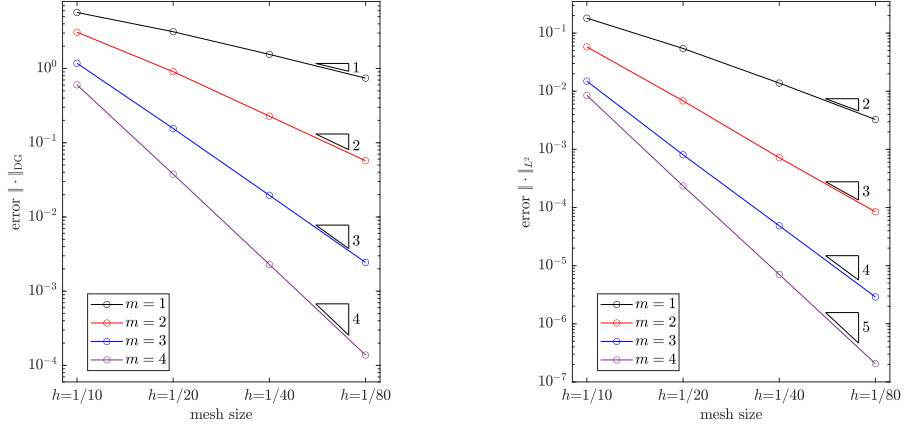


FIGURE 3. The numerical errors under the energy norm (left)/ L^2 norm (right) in Example 1.

We next focus on the resulting linear system arising from the bilinear form (14). The condition numbers to the linear systems and the preconditioned systems for all degrees $1 \leq m \leq 4$ are gathered in Tab. 1. We find that the condition number of A_m grows like $O(h^{-2})$ while the condition number of $A_0^{-1}A_m$ increases very slightly, which are consistent to the results in Theorem 3 and Theorem 4. The iteration counts for standard/preconditioned CG methods are collected in Tab. 2. For both multigrid preconditioning methods, the convergence steps are observed to remain numerically constant as the unfitted mesh is refined, demonstrating the effectiveness to our preconditioning methods.

Furthermore, we show the robustness of the scheme and the preconditioner for the case involving the coefficient with a large jump. We take $\alpha_0 = 10^0, 10^1, \dots, 10^4$. The L^2 errors and the iteration counts for different coefficients on the mesh with $h = 1/40$ are summarized in Tab. 3 and Tab. 4, respectively. Numerical results illustrate that both the errors and the counts are nearly unchanged for all α_0 , which verify the theoretical results 2 and 4.

		h			
		1/10	1/20	1/40	1/80
1	$\kappa(A_0^{-1}A_m)$	15.15	17.29	18.60	19.53
	$\kappa(A_m)$	3.98e+3	1.94e+4	7.56e+4	2.79e+5
2	$\kappa(A_0^{-1}A_m)$	36.87	57.07	64.84	68.66
	$\kappa(A_m)$	5.88e+3	2.92e+4	1.10e+5	3.89e+5
3	$\kappa(A_0^{-1}A_m)$	141.54	168.02	195.39	201.93
	$\kappa(A_m)$	1.67e+4	6.80e+4	2.20e+5	8.58e+5
4	$\kappa(A_0^{-1}A_m)$	385.61	635.56	637.90	644.98
	$\kappa(A_m)$	3.07e+4	1.35e+5	5.39e+5	2.13e+6

TABLE 1. The condition numbers of preconditioned/nonpreconditioned linear systems in Example 1.

m	Preconditioner	h			
		1/10	1/20	1/40	1/80
1	Algorithm 1 for A_0^{-1}	36	40	42	43
	Algorithm 2 for A_0^{-1}	36	40	41	41
	Identity	182	413	758	1707
2	Algorithm 1 for A_0^{-1}	60	65	70	72
	Algorithm 2 for A_0^{-1}	60	64	68	71
	Identity	327	613	1213	2309
3	Algorithm 1 for A_0^{-1}	104	117	123	131
	Algorithm 2 for A_0^{-1}	104	115	123	128
	Identity	612	1209	2361	> 3000
4	Algorithm 1 for A_0^{-1}	190	203	217	227
	Algorithm 2 for A_0^{-1}	190	202	214	223
	Identity	943	1906	> 3000	> 3000

TABLE 2. The iteration counts for PCG/CG solver in Example 1.

m	α_0	10^0	10^1	10^2	10^3	10^4
		1	1.32e-2	1.30e-2	1.22e-2	1.18e-2
2	7.25e-4	7.18e-4	7.18e-4	7.18e-4	7.18e-4	
3	5.26e-5	4.85e-5	4.85e-5	4.86e-5	4.86e-5	
4	7.29e-6	7.07e-6	7.13e-6	7.13e-6	7.13e-6	

TABLE 3. The numerical errors for different α_0 in Example 1.

m	α_0	10^0	10^1	10^2	10^3	10^4
		1	21	22	22	20
2	41	45	43	42	40	
3	83	87	86	89	87	
4	129	132	134	123	120	

TABLE 4. Iteration counts of the PCG solver for different α_0 in Example 1.

Example 2. In this example, we test our method by solving an interface problem with an star-shaped interface consisting of both concave and convex curve segments, see Fig. 1. The interface Γ is governed by the level-set function

$$r = \frac{1}{2} + \frac{\sin 5\theta}{7},$$

in polar coordinates (r, θ) . The analytic solution and the coefficient are taken to be the same as in Example 1. We depict the convergence histories in Fig. 4, which again confirm the theoretical results in Theorem 2. The condition numbers to A_m and $A_0^{-1}A_m$ are presented in Tab. 5, and the iteration counts are listed in Tab. 6. As in Example 1, the condition number of the preconditioned system is nearly constant as the mesh is refined. The iteration counts for both preconditioning methods increase slightly, which agree with the results in Theorem 3 and Theorem 4.

Example 3. In this test, we solve a three-dimensional problem and the interface Γ is a sphere centered at $(0.5, 0.5, 0.5)$ with the radius $r = 0.35$ (see Fig. 2). The exact solution and the coefficient are selected

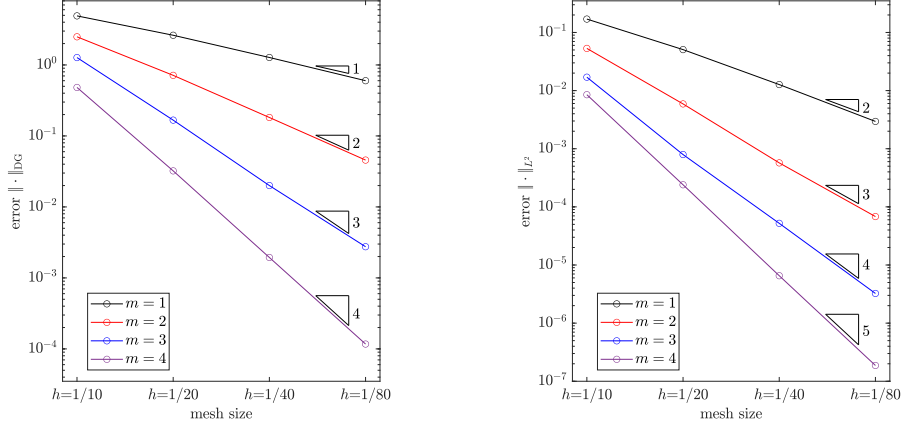


FIGURE 4. The numerical errors under the energy norm (left)/ L^2 norm (right) in Example 2.

		h			
		1/10	1/20	1/40	1/80
1	$\kappa(A_0^{-1}A_m)$	11.57	13.83	15.61	16.77
	$\kappa(A_m)$	2.60e+3	1.06e+4	4.24e+4	1.50e+5
2	$\kappa(A_0^{-1}A_m)$	37.42	48.52	62.48	68.61
	$\kappa(A_m)$	2.48e+3	9.27e+3	4.42e+4	1.55e+5
3	$\kappa(A_0^{-1}A_m)$	106.69	169.07	211.36	243.75
	$\kappa(A_m)$	8.99e+3	3.53e+4	1.29e+5	5.10e+5
4	$\kappa(A_0^{-1}A_m)$	387.42	526.75	675.55	679.57
	$\kappa(A_m)$	1.00e+4	4.34e+4	1.52e+5	6.00e+5

TABLE 5. The condition numbers of preconditioned/nonpreconditioned linear systems in Example 2.

as

$$u(x, y, z) = \begin{cases} \sin(\pi x) \sin(\pi y) \sin(\pi z), & \text{in } \Omega_0, \\ e^{x+y+z}, & \text{in } \Omega_1, \end{cases} \quad \alpha = 1 \quad \text{in } \Omega.$$

The convergence histories are plotted in Fig. 5, and the numerical results demonstrate that the convergence rates under both error measurements are optimal, which confirm the error estimation in three dimensions. The condition numbers and the CG iteration counts for preconditioned systems and nonpreconditioned systems are collected in Tab. 7 and Tab. 8. It can be seen that the condition numbers of the preconditioned linear system are almost constant, and the CG iteration counts increase very slightly. These numerical observations demonstrate the accuracy and the efficiency to our method in three dimensions.

Example 4. In this example, another three-dimensional elliptic interface problem is considered, where the interface is given by the following level set function (see Fig. 2),

$$\phi(x, y, z) = ((2.5(x - 0.5))^2 + (4.2(y - 0.5))^2 + (2.5(z - 0.5))^2 + 0.9)^2 - 64(y - 0.5)^2 - 1.3.$$

The analytic solution and the coefficient are taken to be the same as in Example 3. The numerical results under the energy norm and the L^2 norm are depicted in Fig. 6. The numerically detected

m	Preconditioner	h			
		1/10	1/20	1/40	1/80
1	Algorithm 1 for A_0^{-1}	31	38	40	41
	Algorithm 2 for A_0^{-1}	31	37	39	39
	Identity	348	690	1371	2733
2	Algorithm 1 for A_0^{-1}	51	60	66	70
	Algorithm 2 for A_0^{-1}	51	57	64	67
	Identity	392	766	1540	> 3000
3	Algorithm 1 for A_0^{-1}	90	116	136	144
	Algorithm 2 for A_0^{-1}	90	115	135	143
	Identity	666	1288	2517	> 3000
4	Algorithm 1 for A_0^{-1}	140	185	229	236
	Algorithm 2 for A_0^{-1}	140	184	227	232
	Identity	924	1939	> 3000	> 3000

TABLE 6. The iteration counts for PCG/CG methods in Example 2.

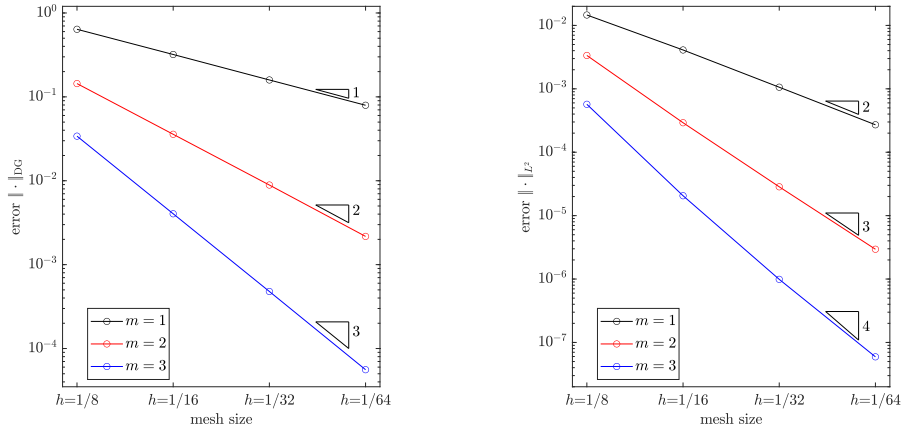


FIGURE 5. The numerical errors under the energy norm (left)/ L^2 norm (right) in Example 3.

convergence rates under both norms are optimal, which match the theoretical analysis. For this test, the condition numbers of the resulting linear systems are shown in Tab. 9. It can be observed that the condition number $\kappa(A_m)$ grows at the speed $O(h^{-2})$, while the condition number $\kappa(A_0^{-1}A_m)$ increases only marginally as the mesh size h tends to zero. In Tab. 10, we list the iteration counts for PCG/CG solvers. In accordance with the condition number, the PCG iteration counts for convergence are numerically observed to be independent of the mesh size.

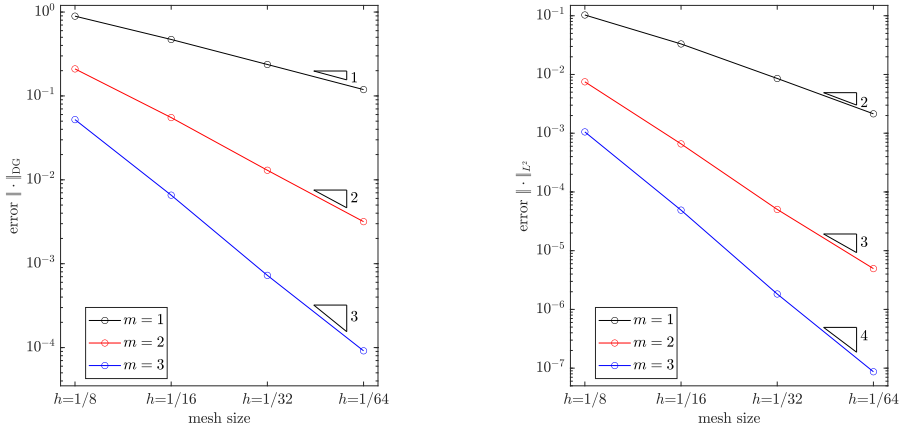
Efficiency Comparison. The main feature of our proposed method is that each element has only one degree of freedom, independent of the degree m . Hughes et al. [28] point out that the number of unknowns for a discretized problem is a reasonable indicator for evaluating the computational efficiency of a numerical method. We make a numerical comparison between the proposed reconstructed method and the unfitted discontinuous Galerkin method [22]. Both methods are tested on Example 1 and Example 3, as the two-dimensional and three-dimensional test cases, respectively. In Fig. 7, we plot the L^2 numerical errors for both methods against the number of degrees of freedom with different

		h			
		1/8	1/16	1/32	1/64
1	$\kappa(A_0^{-1}A_m)$	21.07	31.88	37.99	41.13
	$\kappa(A_m)$	6.879e+2	2.688e+3	1.005e+4	3.603e+4
2	$\kappa(A_0^{-1}A_m)$	86.69	119.04	153.90	162.77
	$\kappa(A_m)$	1.472e+3	5.556e+3	1.944e+4	7.399e+4
3	$\kappa(A_0^{-1}A_m)$	421.56	665.79	707.23	778.74
	$\kappa(A_m)$	3.181e+3	1.162e+4	4.042e+4	1.562e+5

TABLE 7. The condition numbers of preconditioned/nonpreconditioned linear systems in Example 3.

m		h			
		1/8	1/16	1/32	1/64
1	Preconditioner				
	Algorithm 1 for A_0^{-1}	50	58	68	76
	Algorithm 2 for A_0^{-1}	50	57	64	70
	Identity	159	787	1357	2674
2	Algorithm 1 for A_0^{-1}	90	112	125	119
	Algorithm 2 for A_0^{-1}	90	110	121	114
	Identity	109	1005	2052	> 3000
3	Algorithm 1 for A_0^{-1}	172	201	226	235
	Algorithm 2 for A_0^{-1}	172	198	221	224
	Identity	118	1677	> 3000	> 3000

TABLE 8. The iteration counts for PCG/CG methods in Example 3.

FIGURE 6. The numerical errors under the energy norm (left)/ L^2 norm (right) in Example 4.

degrees. It can be seen that in two and three dimensions, the reconstructed method always has better efficiency, in the sense that it uses fewer degrees of freedom to achieve a comparable numerical error. In Tab. 11, we list the ratio of the number of degrees of freedom required by the two methods to reach

		h			
		1/8	1/16	1/32	1/64
1	$\kappa(A_0^{-1}A_m)$	19.68	25.20	31.65	36.98
	$\kappa(A_m)$	6.241e+2	2.259e+3	9.109e+3	3.583e+4
2	$\kappa(A_0^{-1}A_m)$	76.49	103.64	108.37	143.35
	$\kappa(A_m)$	1.205e+3	4.650e+3	1.504e+4	5.910e+4
3	$\kappa(A_0^{-1}A_m)$	385.67	625.88	646.12	720.47
	$\kappa(A_m)$	3.025e+3	1.114e+4	3.4157e+4	1.320e+5

TABLE 9. The condition numbers of preconditioned/nonpreconditioned linear systems in Example 4.

m		h			
		1/8	1/16	1/32	1/64
1	Preconditioner				
	Algorithm 1 for A_0^{-1}	47	55	65	72
	Algorithm 2 for A_0^{-1}	47	54	61	64
	Identity	128	622	1258	2405
2	Preconditioner				
	Algorithm 1 for A_0^{-1}	85	107	115	119
	Algorithm 2 for A_0^{-1}	85	107	114	113
	Identity	101	900	1641	> 3000
3	Preconditioner				
	Algorithm 1 for A_0^{-1}	162	196	211	231
	Algorithm 2 for A_0^{-1}	162	195	208	218
	Identity	110	1449	> 3000	> 3000

TABLE 10. The iteration counts for PCG/CG methods in Example 4.

the same numerical error. The advantage in the approximation efficiency becomes more remarkable for higher-order accuracy.

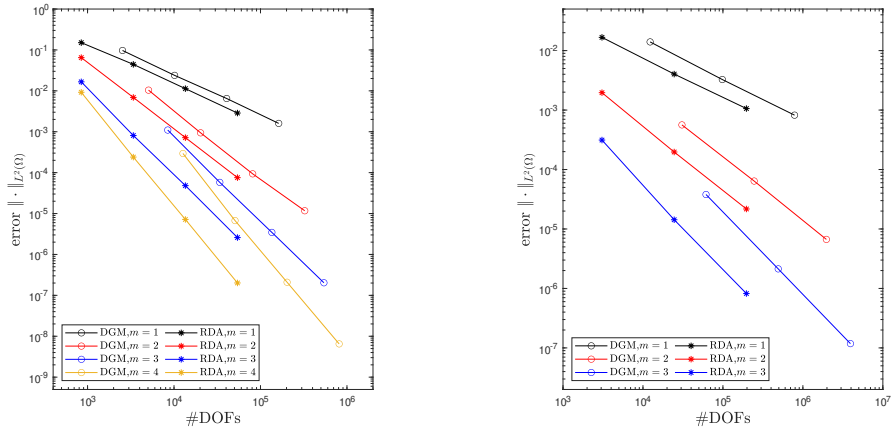


FIGURE 7. The L^2 numerical errors in number of degrees of freedom for RDA/DG methods in two and three dimensions.

m	1	2	3	4
RDA/DG	84%	43%	37%	31%

m	1	2	3
RDA/DG	61%	36%	23%

TABLE 11. The ratio of the number of degrees of freedom involved in RDA/DG methods when achieving a comparable L^2 error in two and three dimensions.

7. CONCLUSIONS

In this paper, we develop a preconditioned unfitted finite element method for the elliptic interface problem, based on the reconstructed discontinuous approximation. The approximation space is constructed by a patch reconstruction process, where each element possesses only one degree of freedom. Thanks to the patch reconstruction, the stability near the interface is naturally ensured, and we prove the optimal convergence rates. Moreover, we construct a preconditioner from the piecewise constant space for the high-order space, and the preconditioned linear system is proven to be optimal and independent of how the interface cuts the mesh. For the lowest-order system, we propose a multigrid algorithm, which can be used as a preconditioner for the high-order system. Numerical experiments in two and three dimensions illustrate the convergence rates of the discretization and the efficiency of the preconditioning method.

APPENDIX A.

Here, we present more details and numerical tests for the constants $\Lambda_{m,K,i}$ and Λ_m . We first briefly introduce their computing methods for a given element patch \mathcal{S}_K^i . For the element $K \in \mathcal{T}_{h,i}$, let p_1, p_2, \dots, p_l be a set of orthonormal basis functions in $\mathcal{P}_m(K)$ under the inner product $(\cdot, \cdot)_{L^2(K)}$. For any polynomial $q \in \mathcal{P}_m(K)$, it can be expressed by coefficients $\boldsymbol{\alpha} = \{a_j\}_{j=1}^l \in \mathbb{R}^l$ that $q = \sum_{j=1}^l a_j p_j$. The polynomials q and p_j can be directly extended to the domain \mathcal{D}_K^i . From the definition (10), the constant $\Lambda_{m,K,i}$ can be equivalently written into an algebraic form,

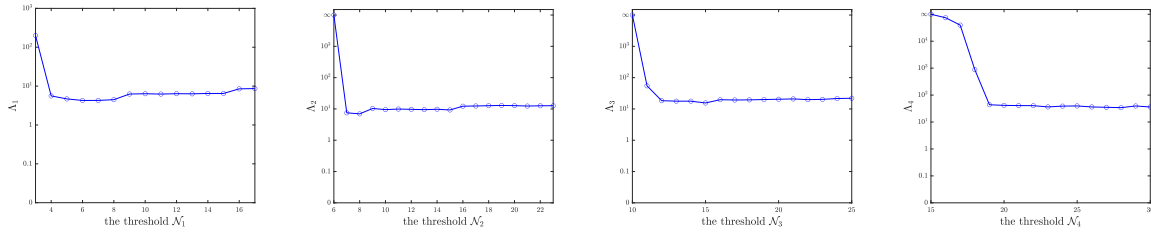
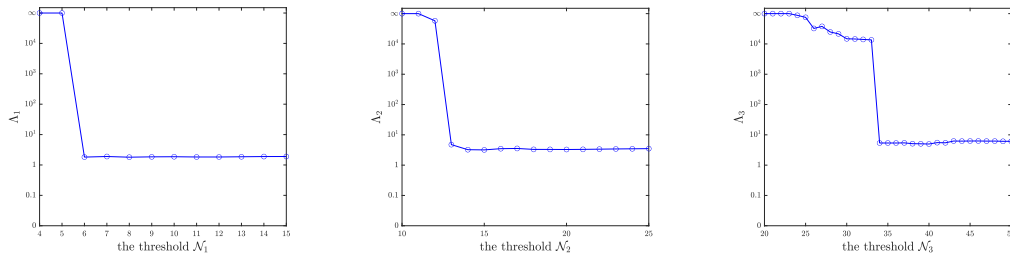
$$\Lambda_{m,K,i}^2 = \max_{\boldsymbol{\alpha} \in \mathbb{R}^l} \frac{|\boldsymbol{\alpha}|_{l^2}^2}{h_K^d \boldsymbol{\alpha}^T B_{K,i} \boldsymbol{\alpha}},$$

where the matrix $B_{K,i}$ is given as

$$B_{K,i} = \{b_{jk}^i\}, \quad b_{jk}^i = \sum_{K' \in \mathcal{S}_K^i} p_j(\mathbf{x}_{K'}) p_k(\mathbf{x}_{K'}).$$

Then, there holds $\Lambda_{m,K,i} = (h_K^d \sigma_{\min}(B_{K,i}))^{-1/2}$, where $\sigma_{\min}(\cdot)$ denotes the smallest singular value for a given matrix. Consequently, the constant Λ_m can be readily obtained by computing the smallest singular value for all $B_{K,i}$.

In Figure 8, we plot the stability constant Λ_m against the given threshold \mathcal{N}_m on the mesh with $h = 1/40$ for degrees $1 \leq m \leq 4$. Here, \mathcal{N}_m is a prespecified parameter that controls the size of the element patch. It is clear that Λ_m is nearly constant when the threshold \mathcal{N}_m is large enough, which verifies the theoretical prediction given in Section 3. From the numerical observation, \mathcal{N}_m is close to $\dim(\mathbb{P}_m) + m + 1$ in two dimensions. In Figure 9, we depict the constant Λ_m against the threshold \mathcal{N}_m in three dimensions with the mesh size $h = 1/16$. Similarly, Λ_m is bounded and increases very slightly if \mathcal{N}_m is larger than a specific value. In three dimensions, the threshold \mathcal{N}_m is approximately $1.5 \dim(\mathbb{P}_m)$. In the computer implementation, we can use the condition $\max_{K \in \mathcal{T}_{h,i}} \Lambda_{m,K,i} \leq 5 \min_{K \in \mathcal{T}_{h,i}} \Lambda_{m,K,i}$ as the criterion to check whether the element patches are appropriate. If this condition is violated, we increase the threshold until it is satisfied.

FIGURE 8. The stability constant Λ_m in two dimensions.FIGURE 9. The stability constant Λ_m in three dimensions.

REFERENCES

1. L. Adams and Z. Li, *The immersed interface/multigrid methods for interface problems*, SIAM J. Sci. Comput. **24** (2002), no. 2, 463–479.
2. R. A. Adams and J. J. F. Fournier, *Sobolev Spaces*, second ed., Pure and Applied Mathematics (Amsterdam), vol. 140, Elsevier/Academic Press, Amsterdam, 2003.
3. N. An and H. Chen, *A partially penalty immersed interface finite element method for anisotropic elliptic interface problems*, Numer. Methods Partial Differential Equations **30** (2014), no. 6, 1984–2028.
4. S. Badia and F. Verdugo, *Robust and scalable domain decomposition solvers for unfitted finite element methods*, J. Comput. Appl. Math. **344** (2018), 740–759.
5. S. Badia, F. Verdugo, and A. Martín, *The aggregated unfitted finite element method for elliptic problems*, Comput. Methods Appl. Mech. Engrg. **336** (2018), 533–553.
6. J. W. Barrett and C. M. Elliott, *Fitted and unfitted finite-element methods for elliptic equations with smooth interfaces*, IMA J. Numer. Anal. **7** (1987), no. 3, 283–300.
7. E. Burman, *Ghost penalty*, C. R. Math. Acad. Sci. Paris **348** (2010), no. 21–22, 1217–1220.
8. E. Burman, M. Cicuttin, G. Delay, and A. Ern, *An unfitted hybrid high-order method with cell agglomeration for elliptic interface problems*, SIAM J. Sci. Comput. **43** (2021), no. 2, A859–A882.
9. E. Burman and P. Hansbo, *Fictitious domain finite element methods using cut elements: II. A stabilized Nitsche method*, Appl. Numer. Math. **62** (2012), no. 4, 328–341.
10. ———, *Fictitious domain methods using cut elements: III. A stabilized Nitsche method for Stokes’ problem*, ESAIM Math. Model. Numer. Anal. **48** (2014), no. 3, 859–874.
11. E. Burman, P. Hansbo, M. G. Larson, and S. Zahedi, *Cut finite element methods*, Acta Numer. **34** (2025), 1–121. MR 4926311
12. Z. Cai, X. Ye, and S. Zhang, *Discontinuous Galerkin finite element methods for interface problems: a priori and a posteriori error estimations*, SIAM J. Numer. Anal. **49** (2011), no. 5, 1761–1787.
13. W. Cao, X. Zhang, Z. Zhang, and Q. Zou, *Superconvergence of immersed finite volume methods for one-dimensional interface problems*, J. Sci. Comput. **73** (2017), no. 2–3, 543–565.
14. N. Chalmers and T. Warburton, *Low-order preconditioning of high-order triangular finite elements*, SIAM J. Sci. Comput. **40** (2018), no. 6, A4040–A4059.
15. Z. Chen and J. Zou, *Finite element methods and their convergence for elliptic and parabolic interface problems*, Numer. Math. **79** (1998), no. 2, 175–202.
16. H. Chu, Y. Song, H. Ji, and Y. Cai, *Multigrid algorithm for immersed finite element discretizations of elliptic interface problems*, J. Sci. Comput. **98** (2024), no. 1, Paper No. 26, 35.

17. T. Cui, W. Leng, H. Liu, L. Zhang, and W. Zheng, *High-order numerical quadratures in a tetrahedron with an implicitly defined curved interface*, ACM Trans. Math. Software **46** (2020), no. 1, Art. 3, 18.
18. A. Ern, A. F. Stephansen, and P. Zunino, *A discontinuous Galerkin method with weighted averages for advection-diffusion equations with locally small and anisotropic diffusivity*, IMA J. Numer. Anal. **29** (2009), no. 2, 235–256.
19. S. Gross and A. Reusken, *Analysis of optimal preconditioners for CutFEM*, Numer. Linear Algebra Appl. **30** (2023), no. 5, Paper No. e2486, 23.
20. R. Guo and T. Lin, *A higher degree immersed finite element method based on a Cauchy extension for elliptic interface problems*, SIAM J. Numer. Anal. **57** (2019), no. 4, 1545–1573.
21. C. Gürkan and A. Massing, *A stabilized cut discontinuous Galerkin framework for elliptic boundary value and interface problems*, Comput. Methods Appl. Mech. Engrg. **348** (2019), 466–499.
22. ———, *A stabilized cut discontinuous Galerkin framework for elliptic boundary value and interface problems*, Comput. Methods Appl. Mech. Engrg. **348** (2019), 466–499.
23. J. Guzmán and M. Olshanskii, *Inf-sup stability of geometrically unfitted Stokes finite elements*, Math. Comp. **87** (2018), no. 313, 2091–2112.
24. A. Hansbo and P. Hansbo, *An unfitted finite element method, based on Nitsche’s method, for elliptic interface problems*, Comput. Methods Appl. Mech. Engrg. **191** (2002), no. 47-48, 5537–5552.
25. P. Hansbo, M. G. Larson, and S. Zahedi, *A cut finite element method for a Stokes interface problem*, Appl. Numer. Math. **85** (2014), 90–114.
26. J. Huang and J. Zou, *Uniform a priori estimates for elliptic and static Maxwell interface problems*, Discrete Contin. Dyn. Syst. Ser. B **7** (2007), no. 1, 145–170.
27. P. Huang, H. Wu, and Y. Xiao, *An unfitted interface penalty finite element method for elliptic interface problems*, Comput. Methods Appl. Mech. Engrg. **323** (2017), 439–460.
28. T. J. R. Hughes, G. Engel, L. Mazzei, and M. G. Larson, *A comparison of discontinuous and continuous Galerkin methods based on error estimates, conservation, robustness and efficiency*, Discontinuous Galerkin methods (Newport, RI, 1999), Lect. Notes Comput. Sci. Eng., vol. 11, Springer, Berlin, 2000, pp. 135–146.
29. A. Johansson and M. G. Larson, *A high order discontinuous Galerkin Nitsche method for elliptic problems with fictitious boundary*, Numer. Math. **123** (2013), no. 4, 607–628.
30. O. A. Karakashian and F. Pascal, *Convergence of adaptive discontinuous Galerkin approximations of second-order elliptic problems*, SIAM J. Numer. Anal. **45** (2007), no. 2, 641–665.
31. R. B. Kellogg, *Higher order singularities for interface problems*, The mathematical foundations of the finite element method with applications to partial differential equations (Proc. Sympos., Univ. Maryland, Baltimore, Md., 1972), 1972, pp. 589–602. MR 0433926
32. C. Lehrenfeld and A. Reusken, *Optimal preconditioners for Nitsche-XFEM discretizations of interface problems*, Numer. Math. **135** (2017), no. 2, 313–332.
33. R. J. LeVeque and Z. Li, *The immersed interface method for elliptic equations with discontinuous coefficients and singular sources*, SIAM J. Numer. Anal. **31** (1994), no. 4, 1019–1044.
34. R. Li, Q. Liu, and F. Yang, *A reconstructed discontinuous approximation on unfitted meshes to $H(\text{curl})$ and $H(\text{div})$ interface problems*, Comput. Methods Appl. Mech. Engrg. **403** (2023), no. part A, Paper No. 115723, 27.
35. ———, *Preconditioned nonsymmetric/symmetric discontinuous Galerkin method for elliptic problem with reconstructed discontinuous approximation*, J. Sci. Comput. **100** (2024), no. 3, Paper No. 88, 32.
36. R. Li, P. Ming, Z. Sun, and Z. Yang, *An arbitrary-order discontinuous Galerkin method with one unknown per element*, J. Sci. Comput. **80** (2019), no. 1, 268–288.
37. R. Li, P. Ming, and F. Tang, *An efficient high order heterogeneous multiscale method for elliptic problems*, Multiscale Model. Simul. **10** (2012), no. 1, 259–283.
38. R. Li, Z. Sun, and F. Yang, *Solving eigenvalue problems in a discontinuous approximate space by patch reconstruction*, SIAM J. Sci. Comput. **41** (2019), no. 5, A3381–A3400.
39. R. Li and F. Yang, *A discontinuous Galerkin method by patch reconstruction for elliptic interface problem on unfitted mesh*, SIAM J. Sci. Comput. **42** (2020), no. 2, A1428–A1457.
40. Ruo Li, Qicheng Liu, and Fanyi Yang, *Preconditioned nonsymmetric/symmetric discontinuous Galerkin method for elliptic problem with reconstructed discontinuous approximation*, J. Sci. Comput. **100** (2024), no. 3, Paper No. 88, 32.
41. Z. Li, *The immersed interface method using a finite element formulation*, Appl. Numer. Math. **27** (1998), no. 3, 253–267.
42. T. Lin, Y. Lin, and X. Zhang, *Partially penalized immersed finite element methods for elliptic interface problems*, SIAM J. Numer. Anal. **53** (2015), no. 2, 1121–1144.
43. H. Liu, L. Zhang, X. Zhang, and W. Zheng, *Interface-penalty finite element methods for interface problems in H^1 , $\mathbf{H}(\text{curl})$, and $\mathbf{H}(\text{div})$* , Comput. Methods Appl. Mech. Engrg. **367** (2020), 113137, 16.
44. T. Ludescher, S. Gross, and A. Reusken, *A multigrid method for unfitted finite element discretizations of elliptic interface problems*, SIAM J. Sci. Comput. **42** (2020), no. 1, A318–A342.

45. E. Neiva and S. Badia, *Robust and scalable h-adaptive aggregated unfitted finite elements for interface elliptic problems*, *Comput. Methods Appl. Mech. Engrg.* **380** (2021), Paper No. 113769, 26.
46. W. Pazner, *Efficient low-order refined preconditioners for high-order matrix-free continuous and discontinuous Galerkin methods*, *SIAM J. Sci. Comput.* **42** (2020), no. 5, A3055–A3083.
47. W. Pazner, T. Kolev, and C. R. Dohrmann, *Low-order preconditioning for the high-order finite element de Rham complex*, *SIAM J. Sci. Comput.* **45** (2023), no. 2, A675–A702.
48. P. Vaněk, M. Brezina, and J. Mandel, *Convergence of algebraic multigrid based on smoothed aggregation*, *Numer. Math.* **88** (2001), no. 3, 559–579.
49. P. Vaněk, J. Mandel, and M. Brezina, *Algebraic multigrid by smoothed aggregation for second and fourth order elliptic problems*, vol. 56, 1996, International GAMM-Workshop on Multi-level Methods (Meisdorf, 1994), pp. 179–196.
50. X. S. Wang, L.T. Zhang, and W. K. Liu, *On computational issues of immersed finite element methods*, *J. Comput. Phys.* **228** (2009), no. 7, 2535–2551.
51. H. Wu and Y. Xiao, *An unfitted hp-interface penalty finite element method for elliptic interface problems*, *J. Comput. Math.* **37** (2019), no. 3, 316–339.
52. F. Yang, *The least squares finite element method for elasticity interface problem on unfitted mesh*, *ESAIM Math. Model. Numer. Anal.* **58** (2024), no. 2, 695–721.

CAPT, LMAM AND SCHOOL OF MATHEMATICAL SCIENCES, PEKING UNIVERSITY, BEIJING 100871, P.R. CHINA
Email address: rli@math.pku.edu.cn

HANGZHOU INTERNATIONAL INNOVATION INSTITUTE OF BEIHANG UNIVERSITY, HANGZHOU 311115, P.R. CHINA
Email address: qc_liu@buaa.edu.cn

SCHOOL OF MATHEMATICS, SICHUAN UNIVERSITY, CHENGDU 610065, P.R. CHINA
Email address: yangfanyi@scu.edu.cn

INSTITUTE OF APPLIED PHYSICS AND COMPUTATIONAL MATHEMATICS, BEIJING 100094, P.R. CHINA
Email address: shuhai@pku.org.cn